THE INTERACTION OF MOLECULES WITH LOW- ENERGY (0 - 30 eV) ELECTRONS

H.H. BRONGERSMA

THE INTERACTION OF MOLECULES WITH LOW- ENERGY (0 - 30 eV) ELECTRONS

PROEFSCHRIFT

TER VERKRIJGING VAN DE GRAAD VAN DOCTOR IN DE WISKUNDE EN NATUURWETENSCHAPPEN AAN DE RIJKSUNIVERSITEIT TE LEIDEN, OP GEZAG VAN DE RECTOR MAGNIFICUS DR P. MUNTENDAM, HOOGLERAAR IN DE FACULTEIT DER GENEESKUNDE, TEN OVERSTAAN VAN EEN COMMISSIE UIT DE SENAAT TE VERDEDIGEN OP MAANDAG 13 MEI 1968 TE KLOKKE 15.15 UUR.

door

HIDDE HERMAN BRONGERSMA

geboren te Leiden in 1940

1968
DRUKKERIJ J. H. PASMANS, 'S-GRAVENHAGE

Promotoren: Prof. Dr. L.J. Oosterhoff
Prof. Dr. J. Kistemaker

Aan mijn ouders
Aan mijn vrouw

Contents

Chapter 1

Introduction and survey

The interaction of electrons with atoms and molecules may give rise to several processes. The work described in this thesis is mainly concerned with electronic and vibrational excitation, ionisation, electron capture and dissociative electron capture. The selection rules for the excitation of electronic energy levels of atoms and molecules by electron-impact depend strongly on the experimental conditions which are used. While for high-energy electron-impact the selection rules are very similar to those for optical excitation (the "Born approximation" is valid), practically all electronic transitions are allowed when low-energy electrons are used. For slow processes it is possible that the incident electron is captured into an empty orbital of the target molecule, and a molecular electron is ejected. This electron exchange may give rise to the formation of a triplet state. These differences in the selection rules provide a powerful incentive for using low-energy electron-impact as a spectroscopic tool. This is further emphasized by the fact that transitions for which the excitation energy is larger than 6 eV are measured just as easily as the lower transitions. In light absorption spectroscopy, on the contrary, it is much more difficult to extend the spectra to the region between 2000 and 500 Å. The considerations given above may create the impression that no preference exists for one transition above the other. This is certainly not the case, but it is often difficult to explain the differences. A discussion of the theory of low-energy collision processes is given in chapter 2.

An energy spectrometer which has been designed to study the collisions of nearly monochromatic low-energy electrons with molecules is described in chapter 3. The apparatus resembles in many aspects the instruments described by Schulz (1958). The spectrometer is particularly suitable for the study of threshold excitations. These are processes where the energy of the incident electrons is just above the excitation energy of the level under investigation. At present excitation spectra of molecules which have, at 150°C, a vapour pressure which is larger than 10^{-2} torr (mm Hg) are easily recorded. Moreover, it is possible to operate the spectrometer at temperatures as high as 350° C which makes it possible to study molecules having a very low volatility at room temperature. Special attention has been paid to the energy calibration as this is often of vital importance for

a correct interpretation of the spectra. An accuracy of 0.05 eV is reached in the present instrument. A highly sensitive detection system for the inelastically scattered electrons enables the use of very small primary beam currents (order of 10^{-9} A). This has the advantage that space charge effects are reduced considerably.

In chapter 4 it is shown that singlet-triplet transitions often belong to the most prominent excitations in the spectra. This is also the case for the aliphatic hydrocarbons for which no previous experimental data on triplet levels are available. Another application of the spectrometer is the determination of electron affinities of molecules and of reactive radicals like H and NH_2. These results have the advantage that they are obtained without any interference of solvent effects.

In order to be able to test the validity of certain approximations in theoretical calculations several absolute measurements of total cross sections (transition probabilities) have been performed (chapter 5). The behaviour of the cross sections as a function of the incident electron energy provides information about the nature of the process which is involved. The accuracy of these determinations is not estimated to be better than 30%. Nevertheless these measurements are considered to be of great importance because no such experimental data are yet available for threshold excitation processes.

At first glance it seems somewhat surprising that although Franck and Hertz initiated as early as 1914 the interest for studying electron-atom collisions still little is known about the types and the cross sections of the transitions which are induced by low-energy electron-impact on molecules. The main reason for the slow development of this field arises from the fact that electrons can produce rotational and vibrational excitations of the ground electronic state as well as electronic excitation. Therefore, when an electron has lost a certain amount of energy during many collisions with molecules it is not known whether the energy loss corresponds to a single electronic excitation or to the sum of several rotational, vibrational and electronical excitations. For this reason the study of molecules requires the use of single-scattering electron beam techniques. This necessitates a much greater sensitivity of the detection system. The recent developments of electronic circuitry and ultra high vacuum techniques have led to a renewed interest in low-energy electron-molecule collisions. The occurrence of these processes in the upper layers of the atmosphere and the reactions to which they lead in plasma chemistry have also greatly stimulated this research.

In the following chapters the concept of cross section is frequently used to indicate the effectiveness of a process. The definition of this conception can be given by considering a beam of electrons of homogeneous energy E passing through a gas containing N molecules/unit of volume.

If an electron is regarded as being lost from the beam when it excites a molecule to the n^{th} state, the loss of intensity of the beam in travelling a further distance δx from the point where its intensity is I is given by

$$\delta I = N Q I \delta x \qquad (1.1)$$

The quantity Q, which has the dimensions of area, is called the total collision cross section of the molecule for excitation to the n^{th} state by electrons of energy E.

Chapter 2

THEORY

2.1. Introduction

The experimental results which are presented in this thesis have been obtained for the interaction of low-energy (1 – 25 eV) electrons with molecules. A striking feature of the spectra is the occurrence of singlet-triplet and other optically forbidden transitions. For some of the observed transitions resonances appear very close to threshold. Often inelastic processes are observed at energies of the incident electron which are far too low to give rise to electronic excitation. These processes which correspond to the vibrational excitation of molecules show a maximum in their cross section for an incident electron energy which is close to the absolute value of the theoretically determined negative electron affinity of the target molecule.

In a collision theory describing the interaction of low-energy electrons with molecules proper allowance should be made for such processes.

2.2. Description of the interaction of low-energy electrons with molecules

Since the introduction of quantum theory a number of methods have been developed to describe collision phenomena. A review of these methods has been given by Mott and Massey (1965), while Burke and Smith (1962) have reviewed the special case of low-energy scattering of electrons by hydrogen atoms. The best known of these methods are the Born approximation, the Born-Oppenheimer approximation, the distorted wave method, the close coupling approximation, the adiabatic theory and the method describing the excitation via the formation of negative ions.

Applications of these theories have mainly been restricted to the interaction of an electron with a hydrogen or a helium atom. Efforts directed towards the calculation of cross sections for the excitation of complex molecules (more than two atoms) have only led to the application of the Born approximation (high-energy scattering of electrons neglecting exchange) to the benzene molecule (Inokuti, 1958; Matsuzawa, 1963; Read and Whiterod, 1965).

In this section the theory for low-energy collisions is discussed in a general way. A formal justification for such a description has been given by Feshbach (1958,1962,1967). The presentation is intended to give a better understanding of the physical significance of several methods and of the cases where it is likely that a given method is a good approximation. It is shown that while the existence of near threshold resonances in the cross section is explained in a natural way by the quantum collision theory, this phenomenon is not explained by a classical theory like the one presented by Gryzinski (1965). The usual Born approximation which assumes a weak interaction between the incident electron and the molecule is only valid for high impact energies. In calculating transition probabilities the initial and final scattered wave functions are approximated by plane waves. This description of the collision is certainly not a realistic one for low-energy electron-molecule collisions where the velocity of the incident electron is about equal or smaller than the velocities of the molecular electrons. A collision theory which is adequate for such low energies should, therefore, take into account the importance of the polarisation of the target molecule by the approaching electron and also the distortion of the plane waves by the molecule. Moreover the wavefunctions should be properly antisymmetrised according to the Pauli principle in order to allow for the exchange among the incident and the molecular electrons.

The distortion of the molecule and the incident and scattered wave can be approximated by a superposition of configurations ("configuration interaction") for the electrons and nuclei. In principle an exact description of the collision phenomena can be obtained by taking into account all configurations which arise from a complete set of orthonormal wavefunctions for the molecule plus an electron. This would be, however, far too complicated for actual calculations. The main problem is therefore to develop experience in choosing the configurations which form the largest contribution to the phenomena. For the excitation of the helium atom to its 2^3S state, for instance, one may use the configuration interaction with the 2^1S, 2^3S, and 2^1P states where the mixing of P states accounts for the polarisability of the atom. Such a procedure is called a close coupling method involving the ground and four excited states. It has been shown by Baranger and Gerjuoy(1957), however, that the threshold behaviour of the $1^1S \rightarrow 2^3S$ transition (Fig. 5.1) can already be explained by configuration interaction with a single state of the He^- ion. Such He^- ions are generally not stable but the lifetimes are long enough to produce sharp resonances in elastic scattering experiments. The wavefunctions ψ_m for such

an unstable ion cannot be exact eigenfunctions since eigenstates have infinite lifetimes. They are the solutions of a perturbed Schrödinger equation

$$(H - W_m)\,\psi_m = R \qquad (2.1)$$

ψ_m is a good approximation of an eigenfunction, however, if the perturbation R is so small that the lifetime of an ion is for example at least of the order of 10^{-14} sec.

For cases where the energy ot an excited state plus an electron at a large distance is very close to the energy of the negative ion it is likely that it is quite general that the polarisation of the target molecule by the incident electron is well accounted for by mixing the wave function with that of the negative ion. In the "adiabatic theory" a comparable result is obtained by computing first the quantum state of the molecule when under the influence of the external charge of the colliding particle. Thereupon the scattering of the projectile by the target molecule in the perturbed state is calculated.

The maxima in the cross section for pure vibrational excitation of molecules may also be described in terms of negative ion formation. For the nitrogen molecule a maximum in the cross section for vibrational excitation is observed near 2 eV. Theoretical calculations show that unstable N_2^- ions should also be formed at this energy, while more than 6 eV is needed for a transition to the lowest electronically excited state. It is therefore reasonable to assume that configuration interaction with the N_2^- ion will give a much better approximation than mixing with the lowest electronically excited state. Chen (1944) using a somewhat modified Feshbach formalism has succesfully calculated the influence of the compound negative-ion states on the vibrational excitation of nitrogen. If only one negative ion state is important (an isolated resonance) the transition matrix $I_o(\gamma,\gamma')$ describing the transition from the incident channel γ' (initial state) to the exit channel γ (final state) is given by

$$I_o(\gamma,\gamma') = T_{\gamma\gamma'} + \frac{\langle\psi_o^-(\gamma)\,|U_o|\,\psi_m\rangle\,\langle\psi_m\,|U_o|\,\psi_o^+(\gamma')\rangle}{E - W_m - R_m} \qquad (2.2)$$

$\psi_o^+(\gamma')$ = wavefunction for the incident channel.

$\psi_o^-(\gamma)$ = wavefunction for the exit channel.

U_o = scattering potential

E = total energy of the system.

The term $T_{\gamma\gamma'}$ represents the direct scattering amplitude.
The energy R_m which arises from the fact that the negative ion is not a stable state and therefore is a complex quantity is related to the half width of the resonance.
The second term on the right hand side can be regarded as an excitation via a negative ion state described by the wavefunction ψ_m. When the denominator is close to zero a resonance in the transition probability is observed. This explains why the maximum in the cross section for vibrational excitation of a molecule is observed at an incident electron energy which is close to the absolute value of the theoretically determined negative electron affinity of the target molecule. For the calculation of electronic transitions a formula similar to (2.1) can be used.

Near threshold resonances have not been observed in helium only. The $X^1\Sigma_g^+ \longrightarrow E^{1,3}\,\Sigma_g^+$ transition of nitrogen at 11,87 eV is also sharply peaked near threshold (Fig.5.3 and 5.4). It is remarkable that Heideman et al. (1966) observe a resonance in the elastic scattering at an incident energy of 11.87 eV. Both effects may be interpreted by assuming a strong mixing with the negative ion.

Besides the quantummechanical description of collision processes several successful efforts have been made to use a classical theory. Generally in such a theory the Coulomb interaction of only one of the atomic electrons with the incident electron is only taken into account. Bauer and Bartky (1965) extended the method of Gryzinski (1965) to calculate the threshold behaviour of excitation for diatomic molecules. At present such a classical theory cannot account for the resonances in the cross section. Therefore the method was applied to the $X\ ^1\Sigma_g^+ \rightarrow B\ ^3\pi_g$ transition in nitrogen which experimentally shows a linear increase of the cross section up to at least 1.6 eV above threshold. Moreover, the fact that the measured relative intensities for the vibrational levels closely resemble the theoretical Franck-Condon factors (section 4.2.2)seems to rule out the possibility that a resonance transition is involved.
The classical theory is in agreement with the observed threshold behaviour but the observed preference for this transition can not be explained. Moreover the experimental cross section is about seven times larger than the theoretical value.

Chapter 3

EXPERIMENTAL PROCEDURES

3.1. General

The method consists essentially of generating a beam of monochromatic low-energy electrons. These electrons enter the collision chamber where they may transfer their energy to the target molecules.
The pressure in the collision chamber is so low, that the mean free path of the electrons is large in comparison to the dimensions of the apparatus. Those electrons which lost practically all of their energy are collected and measured as a current at the trapped electron collector. The trapped-electron apparatus is housed in a clean ultra high vacuum system constructed of stainless steel. A schematic cross section through this part of the electron spectrometer is shown in Fig. 3.1.

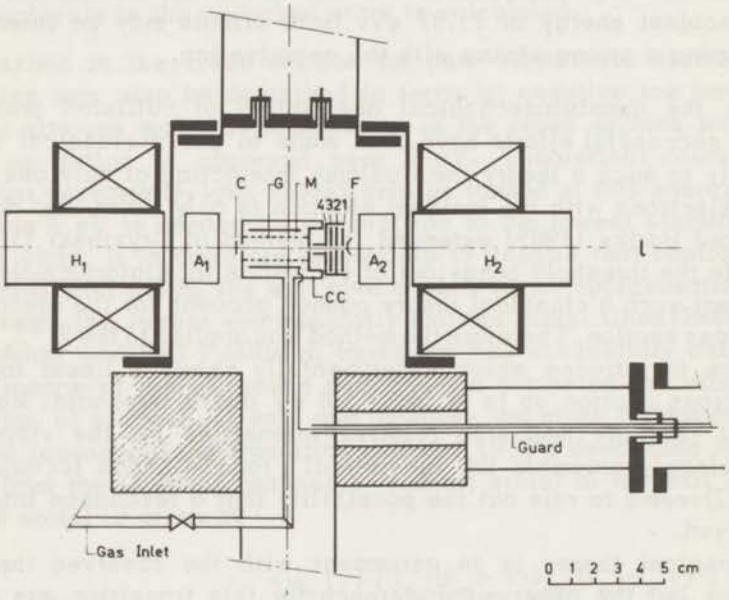

Fig. 3.1. A cross section through the electron spectrometer. F is the filament, 1,2,3 and 4 are electrodes, C is the electron beam collector, G is a cylindrical grid at the same potential as the collision chamber (CC). M is the trapped electron collector, H_1 and H_2 are magnets, A_1 and A_2 are polar pieces. The coordinate l is the axis of the tube.

The electron beam, generated by a Fox electron source (filament F, electrodes 1, 2, 3, and 4) traverses the collision chamber (CC) and is measured at the collector C. Two magnet coils H_1 and H_2 produce a magnetic field. Polar pieces A_1 and A_2 are used to intensify the strength of this field in the collision chamber--maximum 500 gauss--and to facilitate the alignment of the field with the axis of the electrode system. A special configuration of the electrodes effects a potential well in the axial direction of the collision chamber.
The magnetic field prevents the elastically scattered electrons from reaching the trapped electron collector M. Electrons having lost nearly all of their initial energy by an inelastic collision with a target molecule are trapped in the well. This trapping and the diffusion mechanism due to which the trapped electrons can reach the collector M are discussed in section 3.3.1.
Alternatively the energy selection of electrons can be performed by adding a small quantity of an electron scavenger such as SF_6 molecules to the target gas (section 3.4.3.). In the present instrument the trapped electron current is of the order of $10^{-12} - 10^{-16}$ A. This requires the use of a highly-sensitive detection system (section 3.5.).
The vacuum system (Fig. 3.2.) consists essentially of the ultra high vacuum chamber containing the electrode system and of a double inlet system for introducing target gases.
Both parts can be heated by external and internal heating elements. This enables the recording of excitation spectra of liquids and solids of low volatility.
In the apparatus heating, differential pumping and very small electron beam currents generally make the contamination of the electrodes and the influence of space charge negligible.
As a result of these special precautions the resolution of the spectra has been increased considerably.
The use of a double inlet system makes it possible to flow single compounds as well as mixtures through the collision chamber. The importance of this feature for the energy calibration of the spectra is discussed in section (3.6.).

3.2. Vacuum system

A schematic representation of the vacuum system is shown in Fig.3.2. Dotted lines indicate the parts of the apparatus which can be heated. Part 2 is pumped by a 150 l/sec oil diffusion pump (Edwards, type EO 2). The pump is separated from the collision chamber by a water cooled Peltier baffle and a bakeable valve. This enables a simple and continous operation. By using only stainless steel, silver, gold,

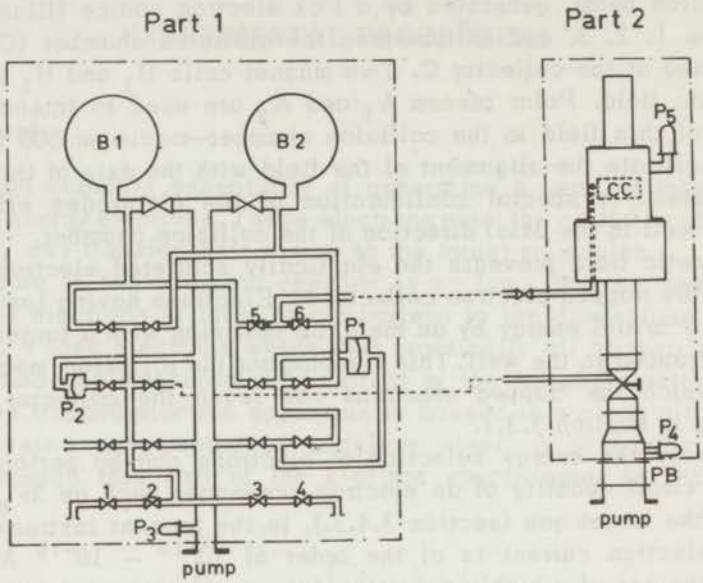

Fig. 3.2. Vacuum system.
Part 1 is the gas inlet system; in part 2 the electron spectrometer is housed. B_1 and B_2 are large spheres for the storage of gases, P_1 and P_2 are membrane gauges, P_3, P_4 and P_5 are ionisation gauges, PB is the Peltier baffle, CC is the collision chamber.

degusit and boron nitride in the construction of the apparatus, a clean vacuum system is obtained in which pressures of the order of 10^{-9} torr are reached. The collision chamber can be baked at 350°C. During the measurements temperatures of 50°C up to 150°C are usually employed for both parts of the apparatus.

Target gases are introduced into the collision chamber via a double inlet system, part 1 (Krupp, type MOL), which is pumped by a 130 l/sec oil diffusion pump (Leybold, type DO 121). The following procedure is used. Gas samples are introduced through valve 1 or 4 and expanded into one of the spheres B. The pressure at which the gas is stored in the spheres is rather high (0.001 up to 10 torr).
When valve 5 or 6 is opened the gas enters the collision chamber through a very small constant leak L and leaves it through the entrance and exit slits. The conductivity of these slits is about 10^3 times as large as that for the leakage L, but is still so small that the pressure

in the electron gun is much smaller than in the collision chamber. Therefore the contamination of the electrodes of the gun will generally be negligible.
The leakage L = 10^{-3} l/sec determines the flow thereby allowing a continuous and reproducible gas flow through the collision chamber. The construction of the leak L and the slits in the collision chamber is that such the requirements for molecular flow are fulfilled. As the flow of a gas under molecular conditions is proportional to $\sqrt{\frac{T}{m}}$, and essentially equal T and temperature molecular weight m are maintained at both sides of the slits the ratio between the pressure in a sphere and the pressure in the collision chamber is independent of the nature of the target gas and the temperature (Rapp and Englander-Golden, 1965).
Once this ratio has been determined it is sufficient to measure only the pressure in the sphere. This can be performed in a routine manner with either of the two membrane gauges P_1 or P_2 (Krupp, types MCT and MMM).

3.3. Fox electron source

The Fox electron gun uses the retarding potential difference (R.P.D.) method to obtain a beam of essentially monoenergetic electrons (Fox, et al. 1955). This method can best be illustrated with the help of Fig.3.3, where a schematic diagram of the potential distribution along the path of the electron beam is shown. The electron source consists of a tungsten filament and four electrodes.
The first electrode (1) extracts the electrons emitted by the filament while electrodes (2) and (4) form an Einzel-lens for focus of the beam. The retarding electrode (3) is operated at a potential V_3, which is slightly negative with respect to the filament. This negative potential is of such a value as to allow the higher energy electrons from the filament to pass the potential barrier while those of lower energy are turned back. The electrons which can pass the potential barrier are accelerated by "the accelerating voltage" V_a and the well depth w. If the retarding potential is changed by a small amount ΔV_3, then the electron distribution will be cut off at a slightly different energy. Effects which are a result of this potential change are due to electrons having an energy between $e(V_a + w)$ and $e(V_a + w + \Delta V_3)$ electron-volts. In practice the potential of the retarding electrode is changed continuously by modulating it with a sine wave generator. From the trapped electron current (I_M) the component which is a result of this modulation is selected and amplified (Fig.3.4). When this amplified

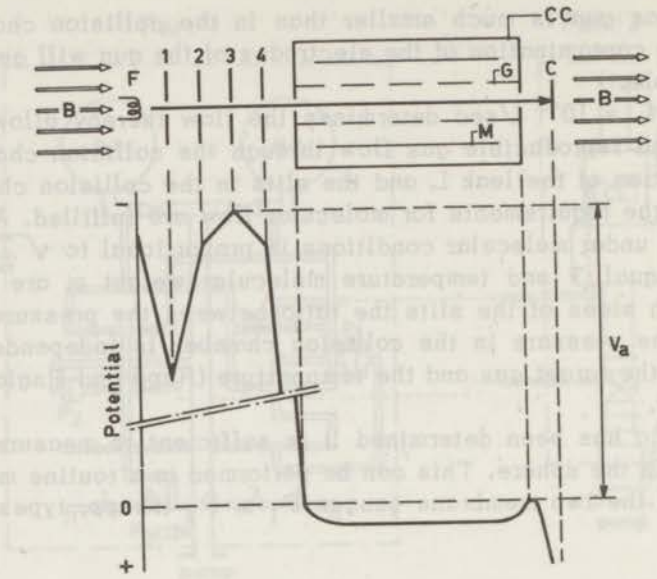

Fig. 3.3. Schematic diagram of the electrode system and the potential distribution along the axis of the tube. B is the magnetic field, V_a the accelerating voltage.

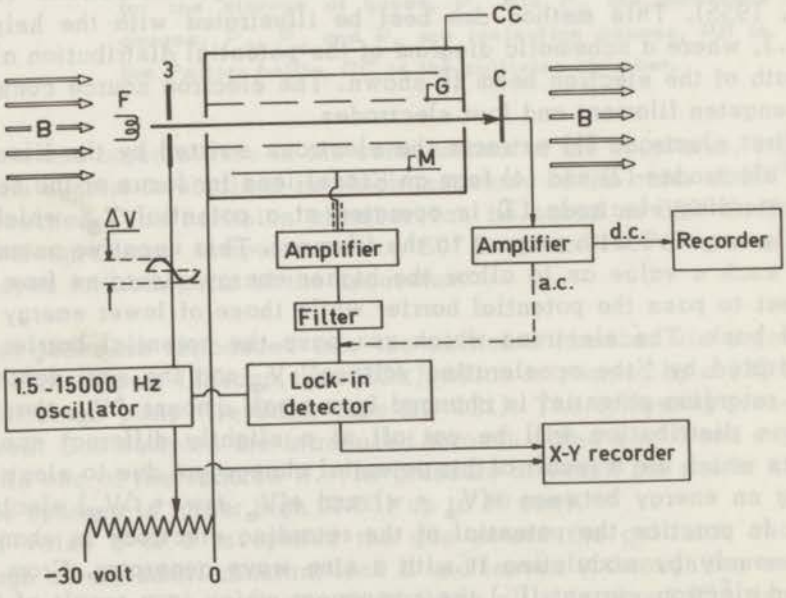

Fig. 3.4. Schematic diagram of apparatus and circuitry.

component is plotted as a function of the accelerating voltage V_a excitation spectra for essentially monoenergetic electrons are obtained. In the present experiment the energy spread of these electrons could be made as small as 0.02 eV.

In the description of the R.P.D. method it has been assumed that acceleration or deceleration has no influence on the energy spread of the electrons. Hartwig and Ulmer (1963), however, point out that this assumption is not always valid. The reason for a change in energy spread is the following. Consider an electron beam which is accelerated by a potential step V_{1z}.
Suppose that before the acceleration the velocity distribution is isotropic around the average velocity v_{oz}. In Fig.3.5B this is illustrated by a sphere in the velocity space.

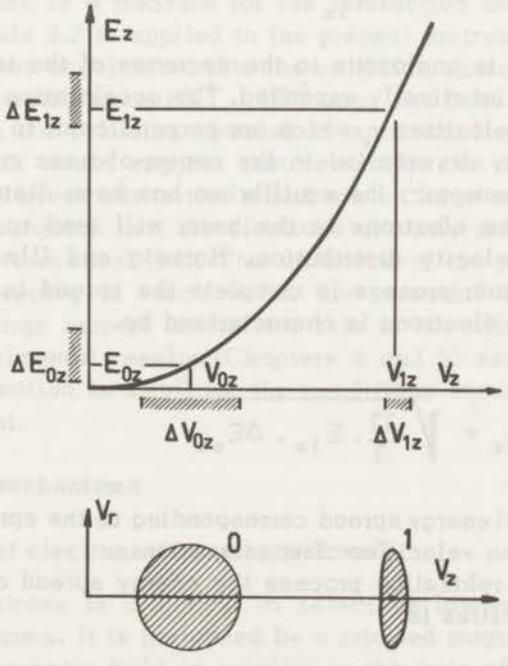

Fig. 3.5. Influence of acceleration in the direction z on the velocity distribution of the electrons.
(A) refers to the direction z.
ΔE_{oz} and ΔE_{1z} are the energy spreads before and after acceleration. Δv_{oz} and Δv_{1z} are the corresponding velocity spreads.
(B) Influence of the acceleration on the velocities v_r perpendicular to v_z.

This sphere is defined as the volume with the smallest surface containing a certain percentage (e.g. 63%) of all the velocity vectors of the electrons. The diameter of the sphere is called the spread (Δv_o) in the velocity before acceleration. The spread in the z component of the velocity (Δv_{oz}) corresponds to a spread in the energy (ΔE_{oz}). When the electrons are accelerated along the z-axis by a potential V_{1z} the energies of the electrons are increased with $E_{1z} - E_{oz} = eV_{1z}$. This has no effect on the energy spread ($\Delta E_{1z} = \Delta E_{oz}$) but the spread in the velocities v_z has been decreased. In Fig.3.5 A this is illustrated with the help of the curve $E_z = 1/2\ mv_z^2$.
For small spreads in the velocity we find

$$\Delta v_{1z} \approx \Delta v_{oz} \cdot \frac{v_{oz}}{v_{1z}} \qquad (\Delta v_{oz} \ll v_{1z})$$

This effect is analogous to the decrease of the temperature of a gas which is adiabatically expanded. The acceleration has no influence on the radial velocities v_r which are perpendicular to the z-axis.
The velocity distribution in the center-of-mass coordinate system is no longer isotropic; the equilibrium has been disturbed. Mutual interaction of the electrons in the beam will tend to establish again an isotropic velocity distribution. Hartwig and Ulmer show that when this relaxation process is complete the spread in the energy distribution of the electrons is characterized by

$$\Delta E_{fz} = \sqrt{\frac{32}{3} \cdot E_{1z} \cdot \Delta E_{oz}} \qquad (3.1)$$

ΔE_{fz} = final energy spread corresponding to the spread in z-components of the velocities after relaxation.
Due to the relaxation process the energy spread corresponding to the radial velocities is

$$\Delta E_{fr} = 2/3\ \Delta E_o$$

ΔE_{fr} = final energy spread corresponding to the spread in the r components of the velocities after relaxation.
In the case of $\Delta E_{oz} = 0.2$ eV and $E_{1z} = 30$ eV this would give rise to $\Delta E_{fz} = 8$ eV
$\Delta E_{fr} = 0.1\bar{3}$ eV.
Fortunately the relaxation time τ is so long that complete relaxation

will not take place in an ordinary electron gun.
Hartwig and Ulmer derive that

$$\tau = \alpha E_o^{-1/2} V_{1z}^{1/6} j^{-1/3} \qquad (3.2)$$

α = factor depending on the geometry of the electron gun and the collision chamber.
E_o = initial energy of the electrons.
V_{1z} = accelerating voltage.
j = current density of the electron beam.

This relaxation process is closely related to the plasma frequency (Lenz, 1960) which is a measure for the interaction among the electrons. When formula 3.2 is applied to the present instrument where the electrons have been accelerated into the collision chamber, the relaxation time is estimated to be $10^{-4} - 10^{-5}$ sec. The time of flightof the electrons through the collision chamber is much smaller (of the order of 10^{-8} sec). This would suggest that relaxation can always be neglected; even for current intensities which are as large as 10^{-5} A/mm^2. However, the assumption that the electrons are only accelerated by a potential step is oversimplified. The influence of the retarding electrode and the trapping of electrons in the potential well has been neglected. For large current intensities this is not allowed (Marmet, 1964). The experimental results (Chapters 4 and 5) suggest that the influence of relaxation is small for the conditions encountered in the present instrument.

3.4. Collection mechanisms

3.4.1. Trapping of electrons in a potential well

Trapping of electrons is a method to select the low-energy from the high-energy electrons. It is performed by a crossed magnetic and electric field. The magnetic field is parallel to the axis of the tube preventing the elastically scattered electrons from reaching the collector M (see Fig.3.3).
A potential well is effected by operating the coaxial cylinder M at a positive potential with respect to the collision chamber. A small fraction of this potential penetrates through the grid G into the center of the tube. This prevents electrons which have lost practically all of their initial energy in an inelastic collision from leaving the collision chamber along the axis (1) of the tube. These electrons will

oscillate until their motion is displaced out of the center of the tube by subsequent collisions. This mechanism by which the electrons can reach the collector M requires many collisions. Therefore notwithstanding the small dimensions of the tube and the low density of the target gas, we can describe this process in terms of a diffusion mechanism.
The time τ for a slow electron to reach the collector M is approximated (Schulz, 1958) by

$$\tau = 0.26 \frac{eB^2R^2}{mV\ \upsilon_c} \qquad (3.3)$$

B = magnetic field
R = radius of the grid G
m = mass of an electron
e = charge of an electron
eV = kinetic energy of the electrons
υ_c = collision frequency of the electrons.

When a spectrum of helium at a pressure of 10^{-3} torr ($\upsilon_c \approx 4.10^{-5}$ collisions/sec) is recorded for a well depth of 0.1 volt and a magnetic field of 200 gauss this would lead for the present instrument to a diffusion time of about 4.10^{-3} sec.

This diffusion mechanism is no longer valid if molecules are studied which have a large attachment coefficient for electrons.
In the extreme case of SF_6 molecules low-energy electrons are captured to form stable SF_6^- ions. Equation 3.3 cannot be used to describe the transport of positive or negative ions to the collector M. For small magnetic fields the ions can reach M directly; for the larger ones only a few collisions are necessary (section 3.4.3). The time which is involved for ions to reach the collector M in the present apparatus is of the order of 10^{-4} sec.
The influence of the potential difference V_{MG} between the collector M and the grid G on the collection efficiency is discussed in section 3.4.4.
A strong magnetic field increases the effectiveness of the energy selection. However, it also increases the diffusion time and thus enhances the formation of space charge in the collision chamber. When primary beam currents of the order of 5.10^{-9} A are used, magnetic fields up to 500 gauss can be employed without creating much space charge.

3.4.2. Determination of the well depth

In chapter 5 it is shown that the trapped electron current due to an excitation process is generally strongly dependent upon the well depth w. An accurate establishment of the well depth is therefore of vital importance for the determination of absolute cross sections. Previous workers (Schulz, 1959; Bowman and Miller, 1965), have described several methods for this determination. However, these do not always lead to the correct result.

Consider an excitation function which is proportional to the excess energy ΔE of the incident electron above the excitation energy eV_e

$$Q = \alpha \Delta E \tag{3.4}$$

Q = cross section for the excitation process
α = proportionality constant.

The electron energy in the collision chamber corresponds to the electron accelerating voltage V_a plus the well depth w. Both V_a and w are positive. In general the well depth, which is only defined at the axis l of the tube, will be a function of l. For simplicity we first assume, however, that the well depth has a constant value. Thus: $w_l = w$. The trapped-electron current will show an onset at $V_a = V_e - w$ (the energy of the electrons in the collision chamber is just equal to eV_e) and then increase linearly with the increase of V_a. Only electrons having an energy less than e w are being trapped. Therefore the excitation curve will decrease abruptly as soon as the condition

$$\Delta E = e\,w \tag{3.5}$$

is reached. In this case: $e\,V_a + e\,w = e\,V_e + \Delta E = e\,V_e + e\,w$, thus

$$V_a = V_e \tag{3.6}$$

The maximum value of the trapped-electron current will be:

$$I_{max} = \int_0^L Q\,I_p\,N\,dl = \alpha I_p\,N\,e\,w\,L \tag{3.7}$$

I_p = primary electron current
N = number of molecules/unit of volume
L = length of the collision chamber.

In practice the shape of the well will not be rectangular but exhibit a form like the curve in Fig.3.3. This will modify the excitation curve somewhat. However, it has no influence on the accelerating voltage for which the peak value is reached. This is true because the condition (3.6) is independent of the depth and the precise shape of the well. The experimental peak shape for an excitation process can be observed in Fig.3.6 for the $1\,^1S \rightarrow 2\,^3S$ transition in helium.

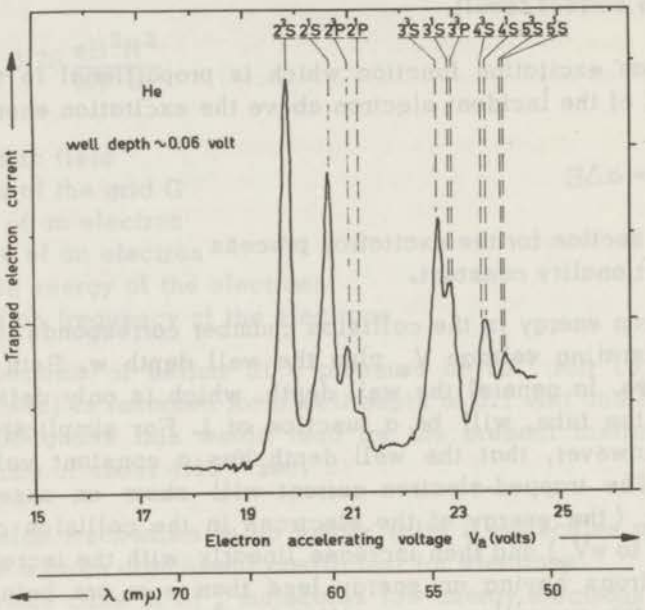

Fig. 3.6. Excitation spectrum of helium.
Optical transition energies are shown above it.
The $1\,^1S \rightarrow 2\,^3S$ transition has been used to calibrate the incident electron energy scale.

The maximum value of the trapped electron current for an arbitrary shape of the well is

$$I_{max} = \int_o^L Q\, I_p\, N\, dl = \alpha I_p\, N \int_o^L w_1\, dl = \alpha I_p\, N\, e\, W\, L \qquad (3.8)$$

W = the average well depth $= \frac{1}{L} \int_o^L w_1\, dl$

The parameter W is therefore important for excitation spectra.

Bowman and Miller (1965) suggest that the well depth can be determined by noting the shift of the 2^3S helium peak as a function of the potential V_{MG}. However, the shift which they observe cannot be a result of the increasing well depth as formula (3.6) shows that the cut off voltage is independent of the well depth.
Possibly the penetration of the voltage V_{MG} through the grid G is such that not only the potential in the center but also that at the end of the tube is changed. This decrease of the threshold at the exit slit would give rise to a shift of the excitation curve.
Schulz (1959) describes other procedures to determine the well depth. These procedures are based on the fact that the influence of a positive value of V_{MG} on the well depth is the same as the influence of a negative value of V_{MG} on the barrier height b_1.

Thus $$\frac{d w_1}{d V_{MG}} = \frac{d b_1}{d V_{MG}}$$

The collector M is operated at a negative potential thus creating a potential barrier. In Schulz's first method the electron current reaching the collector C is plotted as a function of the accelerating voltage V_a for various negative values of V_{MG} (region V_a = 0 volt up to 2 volt). The more negative V_{MG} the higher the accelerating voltage V_a has to be in order that the electrons can pass the potential barrier and reach the collector C.
The top of the barrier determines to what extent the curve is shifted to higher values of V_a. It is found that in the present apparatus

$$\frac{dw_{max}}{d V_{MG}} = \frac{d b_{max}}{d V_{MG}} = 0.19 \pm 0.02 \qquad (3.9)$$

The second method described by Schulz makes use of the influence of V_{MG} on the threshold for positive ion production. This is illustrated with the help of Fig.3.7. Here the shift depends on the average potential barrier B.
The results obtained for the ionisation of carbon monoxide show

$$\frac{d B}{dV_{MG}} = \frac{dW}{dV_{MG}} = 0.16 \pm 0.02 \qquad (3.10)$$

When a target gas is introduced into the collision chamber this gas will partly attach to and (or) dissolve into the grids and electrodes.

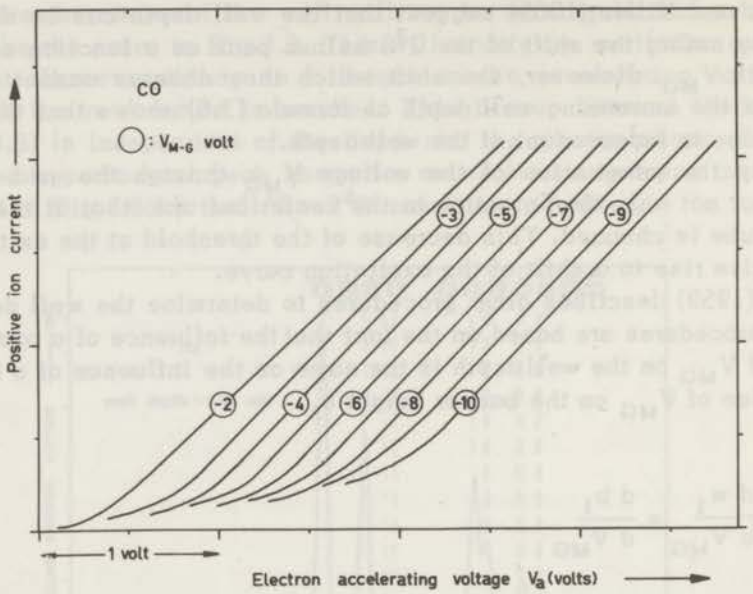

Fig. 3.7. Carbon monoxide.
Influence of the potential difference V_{MG} on the positive ion current vs accelerating voltage.

This may give rise to contact potentials. In order to minimize these effects all non isolating materials have been coated with the same substance, gold. Nevertheless differences between the gas pressure at e.g. the exit slit and at the grid G may give rise to an increase or a decrease of the well.
The influence of this effect can be eliminated. The trapped electron current is plotted as a function of V_{MG} (Fig.3.8).
The extrapolated value of V_{MG} for which the trapped-electron current just reaches zero (V°_{MG}) corresponds to a zero well depth. The average value for the well depth for other values of V_{MG} can now be calculated from the relation

$$W = \frac{d\,W}{d\,V_{MG}} (V_{MG} - V^{\circ}_{MG}) = 0.16\,(V_{MG} - V^{\circ}_{MG}) \qquad (3.11)$$

This relation is independent of the compounds under investigation and provides an easy way for the determination of the average potential well. In all spectra where the well depth is indicated the parameter W is meant.

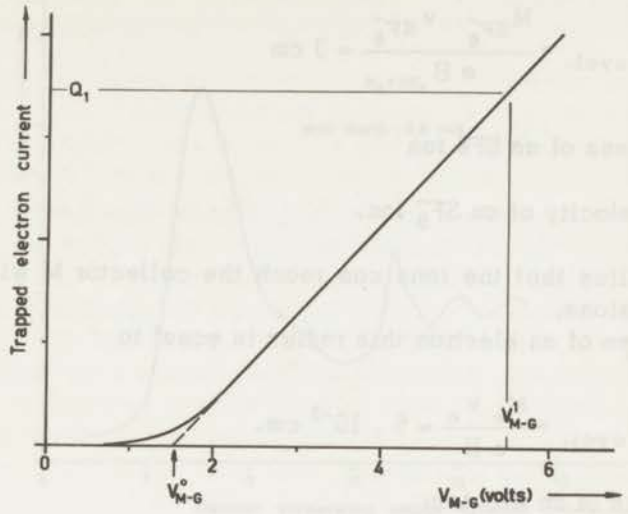

Fig. 3.8. Trapped electron current vs V_{MG} for an arbitrary transition (a linear behaviour near threshold is assumed). V^o_{MG} corresponds to a zero well depth.

The slope near threshold $A = \dfrac{Q_1}{V^1_{MG} - V^o_{MG}}$.

3.4.3. Use of molecules for the energy selection of electrons

Molecules which easily attach electrons of a specific energy can be useful for the energy selection of electrons. An example of such a molecule is SF_6, which captures electrons with energies between 0 and 0.2 eV very efficiently. This process can be either nondissociative or dissociative.

$$e + SF_6 \rightarrow SF_6^-$$

$$e + SF_6 \rightarrow SF_5^- + F$$

The negative ions are, due to their higher mass, less affected by a magnetic field than the electrons.
Consider an SF_6^- ion moving perpendicular to a magnetic field B of 200 gauss. If the velocity corresponds to an energy of 0.2 eV then the ion describes a circular motion with radius

$$R_{cycl.} = \frac{M_{SF_6^-} \; v_{SF_6^-}}{e \; B} \approx 3 \text{ cm}$$

$M_{SF_6^-}$ = mass of an SF_6^- ion

$v_{SF_6^-}$ = velocity of an SF_6^- ion.

This implies that the ions can reach the collector M without making any collisions.
In the case of an electron this radius is equal to

$$R_{cycl.} = \frac{M_e \; v_e}{e \; B} \approx 5 \; . \; 10^{-3} \text{ cm.}$$

M_e = mass of an electron

v_e = velocity of an electron.

Spectra are obtained by mixing the gas under investigation with SF_6 molecules. These spectra show a close resemblance to those recorded for an artificial well depth of approximately 0.2 eV (Fig.3.9 and 3.10). A disadvantage of the method is that electrons are captured over a wide range (0.2 eV), which does not permit the recording of energy spectra with a high resolving power. However, when a mass spectrometer is used to separate the SF_6^- from the SF_5^- ions it should be possible to get much better resolved spectra.
The use of other gases, however, may lead to the selective capture of electrons with a non zero energy. This is of course not possible with a potential well.

3.4.4. Collection of ions

The formation of positive or negative ions can be detected by operating the collector M at a negative or positive potential respectively. The collection efficiency depends not only upon the potential V_{MG} but also on the kinetic energy of the ions.
In the case of non-dissociative electron capture or ionisation

$$e + AB \rightarrow AB^-$$

$$e + AB \rightarrow AB^+ + 2e$$

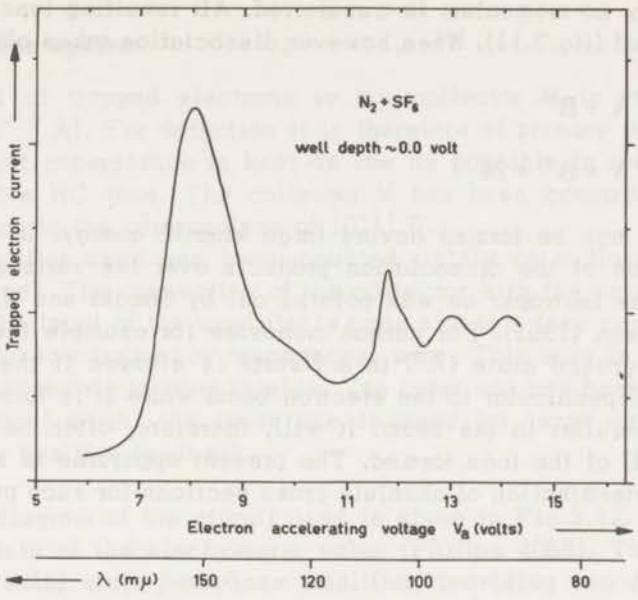

Fig. 3.9. Excitation spectrum of nitrogen. Sulfurhexafluoride molecules have been used for the energy selection of the electrons. The spectrum closely resembles Fig.3.10.

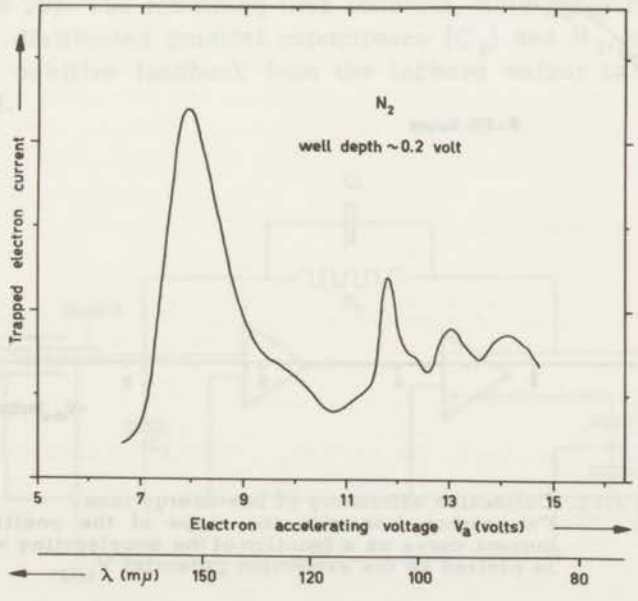

Fig. 3.10. Excitation spectrum of nitrogen using a large well depth.

practically no momentum is transferred. All resulting ions can easily be captured (fig.3.11). When, however, dissociation takes place

$$e + AB \rightarrow A + B^-$$

$$e + AB \rightarrow A + B^+ + 2e$$

particles may be formed having large kinetic energy. In general the distribution of the dissociation products over the various directions will not be isotropic as was pointed out by Sasaki and Nakao (1935) and by Dunn (1962). For carbon monoxide for example the excitation from the ground state (Σ^+) to a Πstate is allowed if the molecular axis is perpendicular to the electron beam while it is forbidden if the axis is parallel to the beam. It will, therefore, often be difficult to collect all of the ions formed. The present apparatus is not suitable for the determination of absolute cross sections for such processes.

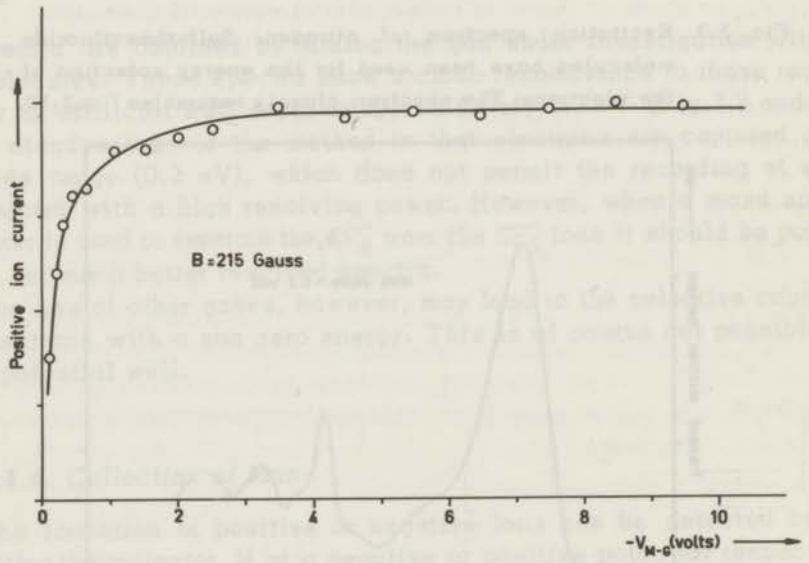

Fig. 3.11. Collection efficiency of low-energy ions.
For carbon monoxide the slope of the positive ion current curve as a function of the accelerating voltage is plotted vs the extraction potential V_{MG}.

3.5. Detection system

The current of trapped electrons to the collector M is very small (10^{-12} – 10^{-16} A). For detection it is therefore of primary importance that the input capacitance is kept as low as possible in order to get an acceptable RC time. The collector M has been constructed with a capacitance to the surroundings of 10^{-11} F.
The preamplifier used has been mounted rigidly on a flange of the vacuum vessel. The connection of the collector with the vacuum feedthrough to the input of the amplifier is made of a thin (low capacitance) tensioned (no low frequency resonances) wire. This wire is surrounded by two concentric tubular shields. The outer one has been connected with signal earth, the inner one is used for input capacitance reduction by positive feedback.

The block diagram of the circuit used is given in Fig.3.12. The first stage consists of the electrometer valve (Philips 4068). The second stage is a solid state paraphase amplifier, providing two outputs of equal amplitude and opposite phase. Using convential negative feedback technique, the current measuring resistance $R_1 = 10^{11}\ \Omega$ (Victoreen Himeg) connects the input with the phase-reversed output. This diminishes the effect of the input capacitance C_1 significantly (some factor 20). The remaining time constant, mainly due to the product of the distributed parallel capacitance (C_2) and R_1, can be decreased by positive feedback from the inphase output to the inner input shield.

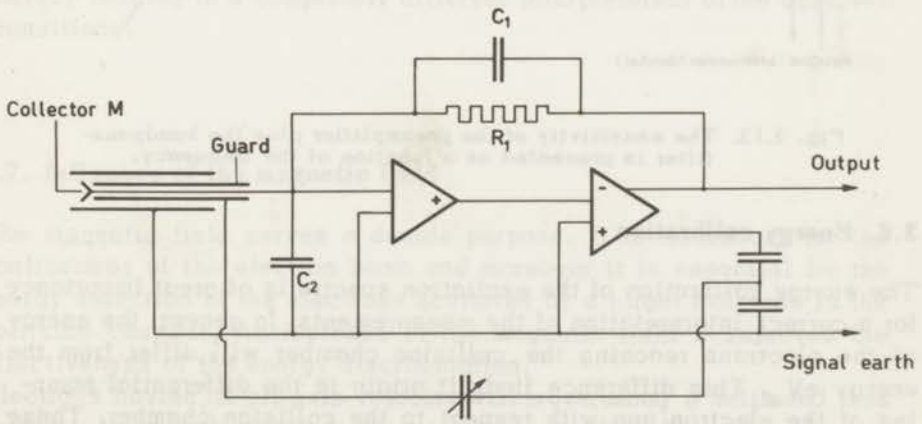

Fig. 3.12. Schematic diagram of the preamplifier and its connection with the trapped-electron collector M.

By keeping the actual amplifier bandwidth reasonably wide, an input timeconstant of a millisecond can be obtained without undue noise or parasitic oscillations. The gain fall-off rate beyond the 3 dB point has a nice 20 dB per decade slope (Fig.3.13). That is why the amplifier remains usable even at 4000 Hz. A modulation frequency of 4 Hz is usually employed.
A tunable bandpass-filter between the preamplifier and the lock-in detector (Princeton Applied Research, JB5) is used to obviate overload of the latter by wideband noise.

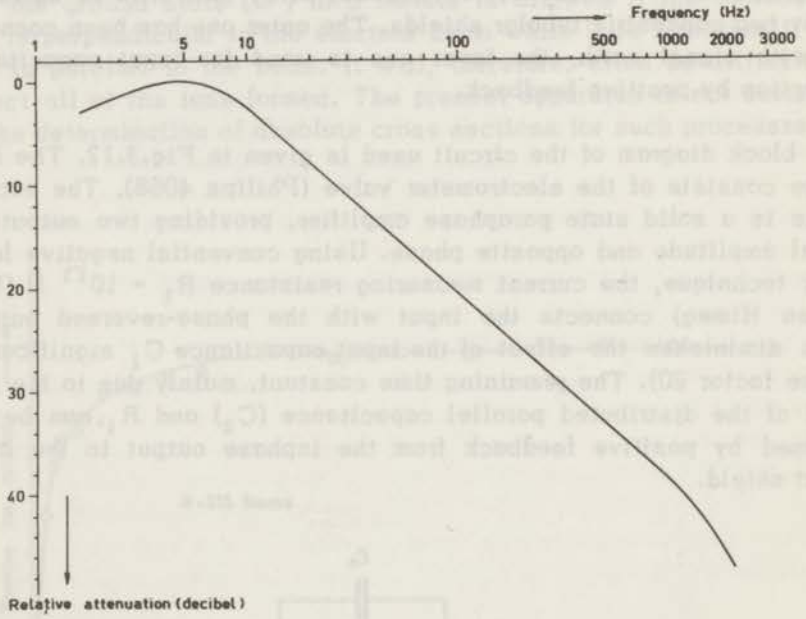

Fig. 3.13. The sensitivity of the preamplifier plus the bandpass-filter is presented as a function of the frequency.

3.6. Energy calibration

The energy calibration of the excitation spectra is of great importance for a correct interpretation of the measurements. In general the energy of the electrons reaching the collision chamber will differ from the energy eV_a. This difference finds it origin in the differential pumping of the electron gun with respect to the collision chamber. These contact potentials are dependent upon the nature and the pressure of the gas introduced. Consequently the contact potentials for the retard-

ing grid electrode 3 and the collision chamber will be different. In order to correct for these potentials the excitation spectrum of a mixture of the compound under investigation and helium is recorded. The $1^1S \rightarrow 2^3S$ transition of helium at 19.82 eV is used to determine the energy shift. This calibration has the advantage that it is performed under the same conditions as the recording of the excitation spectrum of the molecule.
Helium is particularly suitable as a calibration gas because it has no energy levels in the region which is of interest for molecules (1 – 16 eV).
In the usual electron guns where primary electron beam currents of the order of 10^{-4} A are used another type of contact potentials appears due to the attachment of ions formed in the collision chamber to the walls. However, these ions cannot always discharge themselves. This gives rise to surface charging.
In the present instrument this type of contact potentials is relatively unimportant. Small primary electron beam currents (10^{-8} A) give rise to a much smaller number of ions. Moreover all parts of the instrument are gold plated and continuously heated to prevent the formation of isolating layers.
Experimentally it was found that for the same type and pressure of the target gas the contact potential was the same (within 0.1 volt) during a period of one year. This explains why one can accurately calibrate processes with excitation energies as low as 1.3 eV against the helium transition at 19.82 eV (e.g. benzene, Table 4.6).
Schulz (1959) carries out the calibration with helium separately. This explains why his spectrum for nitrogen has to be shifted over 0.3 eV thereby leading to a completely different interpretation of the observed transitions.

3.7. Influence of the magnetic field

The magnetic field serves a double purpose. It is necessary for the confinement of the electron beam and moreover it is essential for the energy selection of the electrons scattered by a target molecule in the collision chamber. An increase of the magnetic field B improves the effectiveness of the energy discrimination.
Electrons having an off-axis velocity will move along a helix and thus increase their path length in the collision chamber. The trapped electron current which is directly proportional to the effective path length

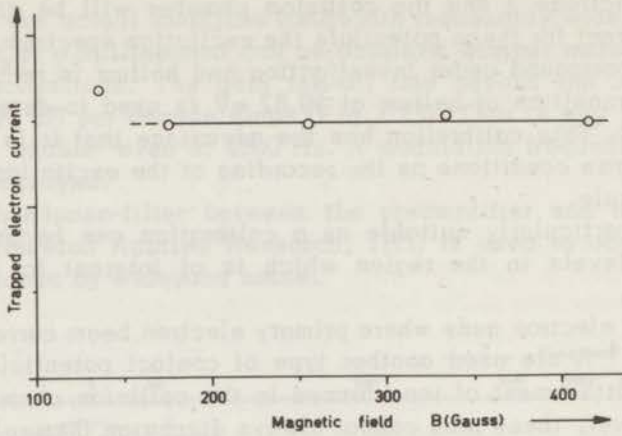

Fig. 3.14. Trapped electron current for the $1\,^1S \rightarrow 2\,^3S$ transition in helium vs the magnetic field.
Below 150 gauss elastically scattered electrons form a large contribution to the total current. An accurate determination of the trapped electron current in this region is therefore impossible. We usually work with 300 gauss.

will therefore depend on B. Craggs, Thorburn and Tozer (1957) had to correct their results for this spiralling motion.
In fig.3.14 it is shown for the $1\,^1S \rightarrow 2\,^3S$ transition in helium that this is not necessary under our experimental conditions.

Chapter 4

MEASUREMENTS AND THEIR INTERPRETATION

4.1. Introduction

The trapped electron method has been used to study several types of electronic transitions in molecules. In particular the transitions in nitrogen and carbon monoxide have been studied carefully because their interpretation is relatively simple. A striking feature of practically all spectra is the importance of singlet-triplet and other optically forbidden transitions. It is believed that this is the first time that singlet-triplet transitions are reported for saturated hydrocarbons. Many examples are presented where electron impact gives rise to processes other than electronic excitation. These processes are: the formation of transient negative ions, dissociative and nondissociative electron capture. From these results electron affinities (in vacuum) and dissociation energies can be determined.

In order to facilitate the comparison of the excitation spectra with the usual ultraviolet and vacuum ultraviolet absorption spectra, a wavelength scale is shown below the spectra. This scale has of course no meaning for processes where the incident electron is captured.

4.2. Nitrogen

4.2.1. Introduction

The interaction of electrons with nitrogen has received much attention in the literature. Rudberg (1930) used a 127° electrostatic energy selector to determine energy-loss spectra of electrons of moderate energy (80 – 587 eV) in nitrogen.
Maier-Leibnitz and Sponer (1934) obtained energy-loss spectra for the near threshold region.
Lassettre and his co-workers (Lassettre et al., 1965[a], 1965[b], 1966; Silverman and Lassettre, 1965[a]; Meyer et al., 1966) have improved the older methods and have recorded well resolved spectra for the energy loss of electrons in nitrogen. In their method the energy loss of electrons scattered at zero angle is measured for incident electron energies of 100 to 500 eV. In these spectra the quadrupole transition $X\ ^1\Sigma_g^+ \rightarrow a\ ^1\Pi_g$ was found besides the optically allowed dipole transitions. Generalized oscillator strengths have been determined for several transitions.

The author wishes to express his gratitude to the Koninklijke/Shell Laboratorium, Amsterdam, who kindly furnished high purity organic compounds.

Recently Skerbele et al. (1967[a]) have succeeded in extending this method to incident electron energies as low as 36 eV. This enabled them to observe weak transitions to triplet levels ($A\ ^3\Sigma_u^+$, $B\ ^3\Pi_g$ and $C\ ^3\Pi_u$).
Heideman et al. (1966) have studied the zero angle scattering of low-energy electrons. They observed very interesting resonance in these transmission measurements, but the higher noise level did not permit the detection of excitation to the $A\ ^3\Sigma_u^+$ or $B\ ^3\Pi_g$ state.
Other authors (Muschlitz et al.,1953; Lichten,1957; Winters, 1965; Olmsted III et al., 1965) determined the total production of metastable molecules by measuring the electrons ejected from a metal surface by such species.
Schulz (1959) and Brongersma et al.(1967[a], 1967[b]) have used the trapped electron method to study the near threshold behaviour of excitation functions. Recently reviews of experimental data have been given by Takayanagi and Takahashi (1966) and by Olmsted III (1967). A comparison of low-energy measurements discloses serious discrepancies among experimental data which lead to large differences of opinion as to their interpretation. It is believed that many of these contradictions are due to an inaccurate calibration of the energy scale.

4.2.2. Discussion of results

Fig.4.1 shows the excitation spectrum of nitrogen obtained for a very small well depth. The most striking features are the transitions between 7 and 9 eV, and the sharp peak at 11.82 eV. In the first band ten vibrational levels show up. The positions of these levels are those to be expected for a transition to the $B\ ^3\Pi_g$ state rather than to the $A\ ^3\Sigma_u^+$ state (Table 4.1). Using the experimental peak shape (taken from the nitrogen peak at 11.8 V or from the $1^1S \rightarrow 2^3S$ transition in helium) to develop the curve it is possible to determine the relative intensities of the vibrational levels. It is found that they are within 10% with the Franck-Condon factors (Benesch et al., 1966) for the $X\ ^1\Sigma_g^+ \rightarrow B\ ^3\Pi_g$ transition. This supports the view that even at these low energies the Franck-Condon principle may hold.
It is surprising that more than 30 years ago Maier-Leibnitz and Sponer (1934) were led by careful experiments to the conviction that the strongest transition near threshold had to be assigned as $X\ ^1\Sigma_g^+ \rightarrow B\ ^3\Pi_g$. This assignment which was proposed in spite of the fact that such a transition is optically forbidden (singlet-triplet; gerade-gerade) has recently been confirmed by Brongersma and Oosterhoff (1967[b]).
The peak at 11.82 eV is assigned as $X\ ^1\Sigma_g^+ \rightarrow E\ ^3\Sigma_g^+ (E\ ^1\Sigma_g^+)$. The 9.5 – 11 eV region does not allow of any definite assignments.

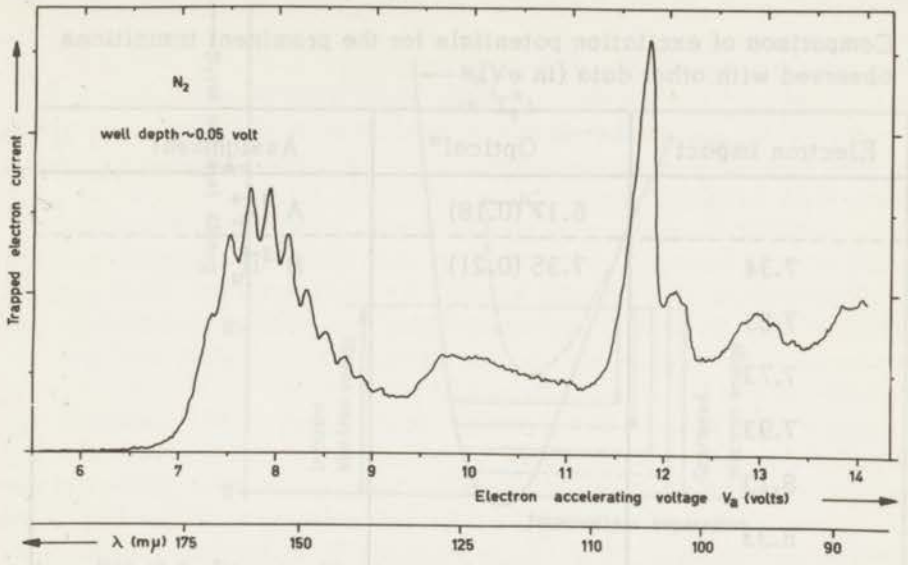

Fig. 4.1. Excitation spectrum of nitrogen.

It seems reasonable that transitions to the $^3\Delta_u$, a $^1\Sigma_u^+$ and w $^1\Delta_u$ state are important. In any case it is not likely that these bands represent transitions to the a $^1\Pi_g$ state. When spectra are recorded for larger well depths the resolution is much lower. Consequently it cannot be excluded that the cross section for the excitation to the a $^1\Pi_g$ state at, for example, 0.2 eV above threshold amounts to about 20% of the corresponding cross section for the B $^3\Pi_g$ state.
For larger well depths a new peak shows up between 1.8 and 3.5 eV (Fig.4.3) which is far below the first electronically excited level, the A $^3\Sigma_u^+$ state at 6.12 V. Experimental results regarding this process date back as early as 1927 (Harries).
Schulz (1962[a]), Schulz and Koons (1966), and Heideman et al.(1966) were able to observe pronounced resonances in the elastic scattering for this region. Schulz (1958) proposed that the process is due to the formation of temporary negative ions

$$N_2 \xrightarrow{e} (N_2^-) \longrightarrow e + N_2(+ \text{ vibrational energy})$$

The well depth which is used for the recording of a spectrum determines the maximum kinetic energy of the electrons which are trapped.

Table 4.1 Nitrogen

Comparison of excitation potentials for the prominent transitions observed with other data (in eV).

Electron impact	Optical[a]	Assignment
	6.17 (0.18)	$A\ ^3\Sigma_u^+$
7.34	7.35 (0.21)	$B\ ^3\Pi_g$
7.53		
7.73		
7.93		
8.13		
8.33		
8.52		
8.72		
(8.90)		
(9.08)		
9.5 – 11.5		$^3\Delta_u$, a $^1\Sigma_u^+$, w $^1\Delta_u$
11.82	11.87	$E\ ^{1,3}\Sigma_g^+$
12.15	11.09; 12.21	$C'\ ^3\Pi_u$; i ?
(12.45)	12.45	$j\ ^1\Sigma_u^+$?
12.86	12.85	$b\ ^1\Sigma_u^+$?
(13.35)		
(13.80)		
13.90		
14.03		

a. Herzberg (1950).
For the $A\ ^3\Sigma_u^+$ and $B\ ^3\Pi_g$ excitation the transition to the lowest vibrational level is given with the vibrational energy splitting in parentheses.

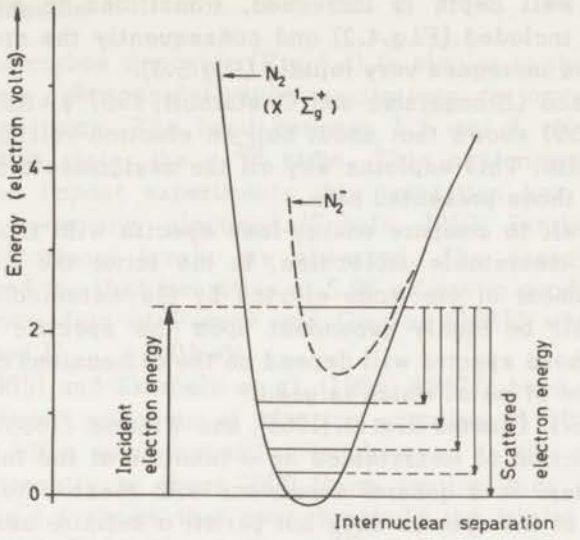

Fig. 4.2. Diagram illustrating the formation of transient negative ions in nitrogen.

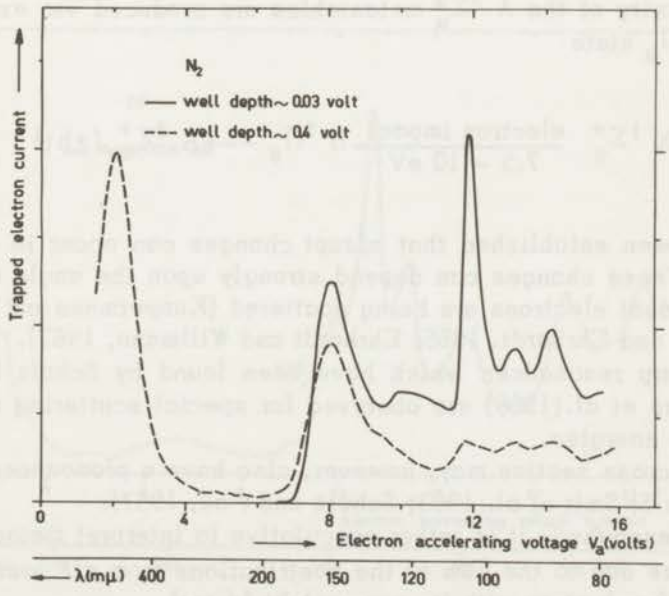

Fig. 4.3. Influence of the well depth on the excitation spectrum of nitrogen.
The energy spread of the incident electrons is too large to observe the vibrational fine structure. The relative intensities of the spectra are arbitrary.

When the well depth is increased, transitions to more vibrational levels are included (Fig.4.2) and consequently the cross section for this process increases very rapidly (Fig.5.3).
A comparison (Brongersma and Oosterhoff, 1967[b]) with the results of Schulz (1959) shows that about half an electron-volt has to be added to his results. This explains why all the assignments given by Schulz differ from those presented here.
It is difficult to compare energy-loss spectra with those for the production of metastable molecules. In the latter the lifetime and the average number of electrons ejected by the metastable from a metal surface will be highly dependent upon the specific excited level. Moreover these spectra will depend on the dimensions of the apparatus and the type of metal which is used.
Lichten (1957), Olmsted III et al. (1965), and Winters (1965) measured the total production of metastables as a function of the incident electron energy. There is a general agreement with these data. However, the resolution of the spectra does not permit a definite assignment of the transitions observed. The linear increase of metastables which they observe in the 7.5 – 10 eV region is consistent with the data shown in chapter 5 for the $B\ ^3\Pi_g$ excitation. This shows that near threshold the majority of the $A\ ^3\Sigma_u^+$ metastables are produced via excitation of the $B\ ^3\Pi_g$ state

$$X\ ^1\Sigma_g^+ \xrightarrow[7.5-10\ eV]{\text{electron impact}} B\ ^3\Pi_g \longrightarrow A\ ^3\Sigma_u^+ \ (+h\upsilon)$$

It has been established that abrupt changes can occur in cross sections. These changes can depend strongly upon the angle over which the incident electrons are being scattered (Kuppermann and Raff, 1963[b]; Andrick and Ehrhardt, 1966; Ehrhardt and Willmann, 1967).
The sharp resonances which have been found by Schulz (1964[b]) and Heideman et al. (1966) are observed for special scattering angles and electron energies.
A total cross section may, however, also have a pronounced structure (Chapter 5; Smit et al., 1963; Schulz and Fox, 1957).
As a consequence it is rather speculative to interpret metastable data which are due to the sum of the contributions from all possible metastables (each state with its own weight factor).
This emphasizes our lack of knowledge of the behaviour of cross sections near threshold.

4.3. Carbon monoxide

The spectrum of carbon monoxide (Fig.4.4) is similar to that obtained for nitrogen. Here again singlet-triplet excitations are among the most pronounced transitions. The band between 5.5 and 7 eV is due to the lowest triplet state, the a $^3\Pi$ state. This assignment explains why in electron impact experiments this transition has only been observed with low-energy electrons (Schulz, 1959; Skerbele et al., 1967[b]). Six vibrational levels are observed. The energy splitting ΔE = 0.21 eV and the first transition at 5.96 eV are in good agreement with fluorescence data of Pearse and Gaydon (1965) who obtained ΔE = 0.20 eV and E_{o-o} = 6.01 eV.
Meyer et al. (1965) and Skerbele et al. (1966, 1967[b]) have determined the electron impact spectrum at electron energies of 50, 200, and 400 eV. At 50 eV a weak transition is observed to the a $^3\Pi$ state, however, its intensity is about 2000 times smaller than that of the A $^1\Pi$ state. Fig.4.4 shows that near threshold the triplet excitation is highly favoured. Excitation to the a $^3\Pi$ state is at least 10 times as important as excitation to the corresponding singlet state. Olmsted III

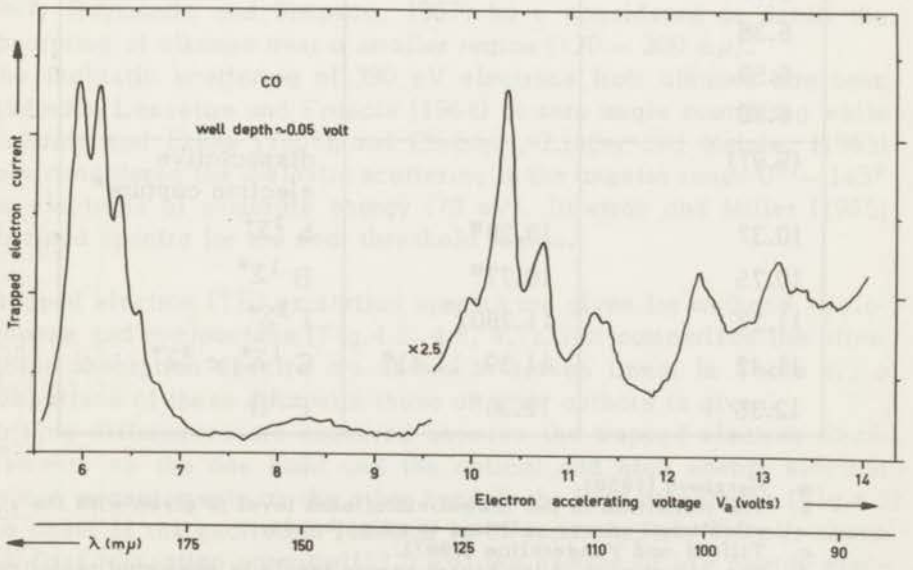

Fig. 4.4. Excitation spectrum of carbon monoxide.
For the right hand side of the spectrum the sensitivity of the detection system has been increased by a factor 2.5.

et al. (1965) studied the production of metastables. However, the short lifetime ($\sim$ 10 μsec) of the a $^3\Pi$ metastables made it difficult to detect this species. A small peak which shows up at 9.97 eV is due to the dissociative electron capture of carbon monoxide

$$CO \xrightarrow[\sim 10\ eV]{\text{electron impact}} C + O^-$$

The intensity of this peak cannot be compared with the other intensities of the spectrum as the well depth is not large enough to collect

Table 4.2 Carbon Monoxide

Comparison of excitation potentials for the prominent transitions observed with other data (in eV).

Electron impact	Other authors	Assignment[d]
5.96	6.01[a] (0.21)[b]	a $^3\Pi$
6.17		
6.38		
6.59		
6.78		
(9.97)		dissociative electron capture[e]
10.37	10.39[a]	b $^3\Sigma^+$
10.75	10.77[a]	B $^1\Sigma^+$
11.27	11.280[c]	j $^3\Sigma^+$
11.42	11.39; 11.41[a]	C $^1\Sigma^+$; c $^3\Sigma^+$
12.35	12.36[a]	F $^1\Pi$

a. Herzberg (1950).
b. The transition to the lowest vibrational level is given with the vibrational energy splitting in parentheses.
c. Tilford and Vanderslice (1967).
d. The assignment of the higher energy levels is somewhat tentative.
e. This peak is due to the process $CO \xrightarrow{e} C + O^-$.
Values obtained for this transition by other authors:

10.1 eV (Craggs and Tozer, 1958)
10.1 eV (Schulz, 1962[b])
9.9 eV (Rapp and Briglia, 1965).

all the O^- ions formed. Craggs and Tozer (1958), Schulz(1962[b]), and Rapp and Briglia (1965) have studied this process. Determinations of the energy for which a maximum in the cross section for dissociative attachment is reached range from 9.9 up to 10.1 eV.
Tilford and Vanderslice (1967) obtained from vacuum ultraviolet absorption spectra a triplet level at 11.280 eV which was identified as the j $^3\Sigma^+$ state. This is in entire agreement with the peak at 11.27 eV presented here.
A comparison of the present experimental results with those of the other authors is shown in Table 4.2.

4.4. Saturated hydrocarbons

The excitation of electronic states in alkanes has received relatively little attention in the literature. This has, in general, been due to difficulties encountered in the recording of ultraviolet absorption spectra for the region where these saturated hydrocarbons absorb (below 180 mμ).
Ditchburn (1955), and Sun and Weissler (1955) studied the light absorption of methane down to wavelengths as short as 35 mμ, while other authors (Moe and Duncan, 1952; Lombos, Sauvageau and Sandorfy, 1967; Raymonda and Simpson, 1967) have considered in detail the absorption of alkanes over a smaller region (120 – 200 mμ).
The inelastic scattering of 390 eV electrons from alkanes has been studied by Lassettre and Francis (1964) at zero angle scattering while Ehrhardt and Erbse (1963), and Ehrhardt, Linder and Meister (1965) have considered the inelastic scattering in the angular range 0° – 145° for electrons of moderate energy (70 eV). Bowman and Miller (1965) obtained spectra for the near threshold region.

Trapped electron (TE) excitation spectra are given for methane, cyclopropane and cyclooctane (Fig.4.5, 4.6, 4.7). For comparison the ultraviolet absorption spectra are shown in broken lines. In Table 4.3 a comparison of these data with those of other authors is given.
Striking differences are observed between the trapped electron measurements on the one hand and the optical and high energy electron impact measurements on the other hand. In the case of methane (Fig.4.5) the onset of the excitation function is at approximately 7.5 eV; above the first ionisation potential(13.0 eV) the number of low energy electrons increases rapidly.
In the high-energy electron-impact and optical spectra the onset is always at 8.5 eV. Furthermore the cross section (absorption) decreases in the region 13 – 16 eV.

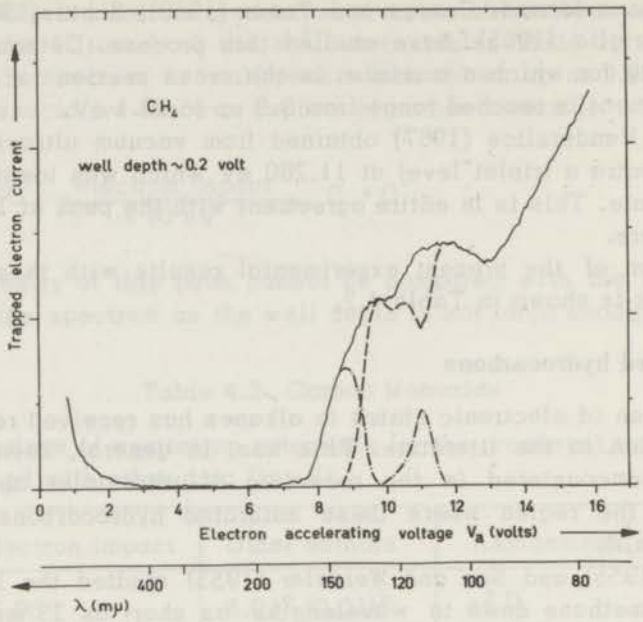

Fig. 4.5. Methane.
The relative intensities of the peaks at ~9.8 and 11.7 eV are the same for the optical, the low-energy and the high-energy electron impact data (Table 4.3). This suggests that for all spectra the same transitions are involved at these energies.
Tentatively the optical excitation spectrum (----, Raymonda and Simpson, 1967) has been normalized to the trapped electron spectrum (——). It is likely that the difference of the spectra (-.-) is a result of singlet-triplet and (perhaps) other optically forbidden transitions.

The difference in onset is far too large to be the result of an inaccurate energy calibration. Moreover Bowman and Miller (1965) using the TE method reported the same value (7.5 eV), but do not seem to have noted this divergency. At moderate energy (70 eV; 3° scattering) a very small cross section has been observed for the 7.5 – 8.5 eV region by Ehrhardt et al. (1965), but no explanation is given of this feature. In the cases of cyclopropane and cyclooctane a similar displacement of the absorption threshold to lower energies is observed in the TE spectrum. It seems plausible to assume that singlet-triplet transitions are involved.
The difference which is encountered in the region between the first and the second (19.5 ± 0.2 eV; Ehrhardt and Linder, 1967) ionisation

Table 4.3 *Saturated hydrocarbons*

A comparison of onset and peak energies (in eV), of this research with other data.
Relative intensities in parentheses.

Molecule	Electron impact				Light absorption	Assignment
	this research	other authors				
methane		1.9–3[a]				transient negative ions
	7.5	7.5[b]	8.5[c]	(7.5–)8.5[d]	8.5[e]	onset
	[8.8]					triplet state
	9.7–10.2(0.78)	9.8(0.73)[b]	10.12(0.79)[c]	9.8(0.94)[d]	9.6; 10.5[e]	
	[11.0]					
	11.7 (1.00)	11.7(1.00)[b]	11.8 (1.00)[c]	11.7(1.00)[d]		
	13.1	13.1[b]	13.27(1.28)[c]	13.1(1.11)[d]	12.99[f];13.16[g]	ionisation
cyclopropane	5.9				7.0[e]	onset
	7.4				7.8[e]	
	9.7				8.6[e]	
	10.1				10.1[e];10.09[f]	ionisation
cyclooctane	6.0				7.0[e]	onset
	7.6					
	[8.5]					
	[8.9]					ionisation

a. Boness et al. (1967).
b. Bowman and Miller (1965).
c. Lassettre and Francis (1964).
d. Ehrhardt, Linder and Meister (1965).
e. Raymonda and Simpson (1967).
f. Watanable (1957).
g. Frost and Mc Dowell (1957).

potential is a result of the increasing ionisation cross section above threshold. Moreover, the contribution of excitation of optically forbidden double excited states to the total cross section may be important

$$CH_4 \xrightarrow[\text{energy above 13 eV}]{\text{electron impact}} CH_4^* \longrightarrow \begin{cases} CH_3^+ + H^- \\ CH_4^+ + e \end{cases}$$

Such an interpretation is in agreement with the measurements of Melton and Hamill (1964) who studied appearance potentials for the formation of positive and negative ions from methane by electron impact in a mass spectrometer.

Boness et al. (1967) observed a weak structure in the transmission spectra of low-energy electrons (1.9 – 3 eV) through methane which was ascribed to the formation of virtual negative ion states. Efforts

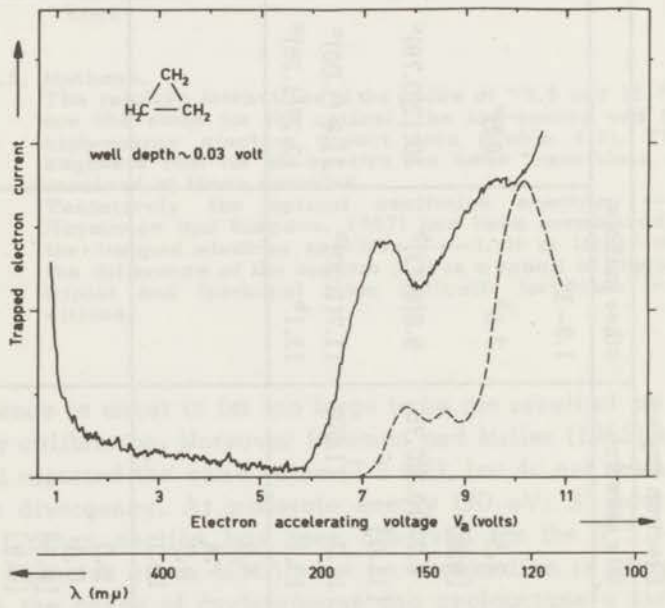

Fig. 4.6. Cyclopropane.
—— trapped electron spectrum.
------ optical excitation spectrum (Raymonda and Simpson, 1967).
The relative intensities of the spectra are arbitrary.

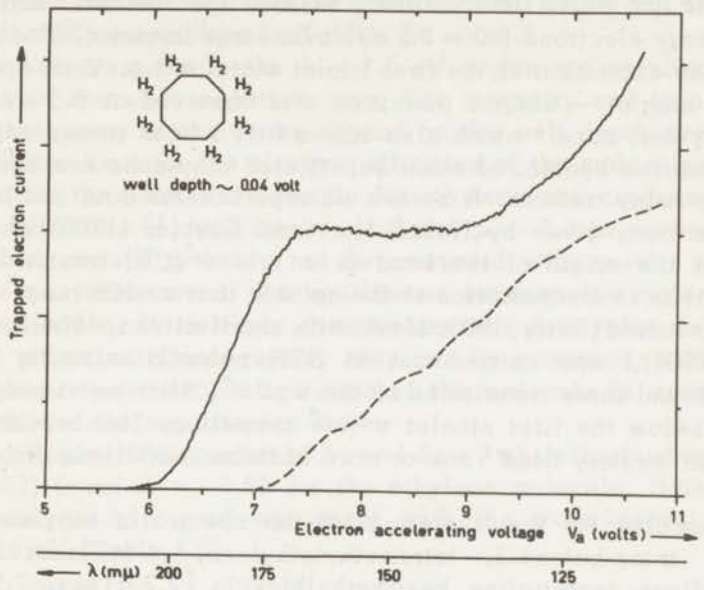

Fig. 4.7. Cyclooctane.
——— trapped electron spectrum.
------ optical excitation spectrum (Raymonda and Simpson, 1967).
The relative intensities of the spectra are arbitrary.

have been made to detect the formation of these transient ions using the TE method. Surprisingly even for a well depth as large as 1.6 volt no indication for the excitation of such a state was found. Of course it is possible that the contribution to the total cross section is so small that it cannot be distinguished from the elastically scattered electrons.

4.5. Olefins

Ethylene is the most extensively studied molecule reported in literature.

Zero angle electron impact spectra of ethylene have been recorded by Simpson and Mielczarek (1963), Geiger and Wittmaack (1965), and Ross and Lassettre (1966). In the spectra of the latter four authors the energy resolution is nearly as good as in the corresponding light absorption spectrum of Zelikoff and Watanable (1953).

Kuppermann and Raff (1963[a], 1963[b]) studied the inelastic scattering of low-energy electrons (40 – 75 eV) over large angles (22° – 112°). Besides the excitation of the first triplet state at 4.4 eV an optically forbidden singlet – singlet transition was observed at 6.5 eV. This "olefin mystery band" which also appears as a weak transition in the light absorption spectra of some substituted ethylenes has been discussed by many authors. A review of experimental data and assignments has been given by Robin, Hart and Kuebler (1966) who conclude that the origin of the band is a $\pi \rightarrow \sigma^*(CH)$ transition. This assignment is in contradiction to the opinion that a $\sigma(CH) \rightarrow \pi^*$ transition is involved (Berry, 1963; Moskowitz and Harrison, 1964). Berthod (1966), who carried out an SCF calculation using Slater orbitals, found three transitions of the $\pi \rightarrow \sigma^*(CH)$ type at excitation energies below the first singlet $\pi \rightarrow \pi^*$ transition. Thus speaking of the "olefin mystery band" one or more of these transitions are meant.

While searching for the mystery band the spectra of ethylene, cis-butene-2, trans-butene-2, tetramethylethylene, 1,4-cyclohexadiene, 1,6-heptadiene, isotetraline, hexamethylbicyclo [2,2,0] hexa-2,5-diene and norbornadiene were recorded (Fig.4.8 – Fig.4.16).

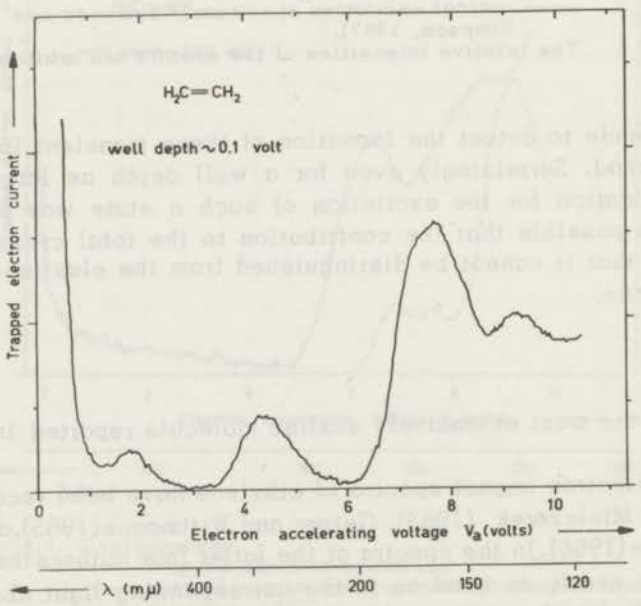

Fig. 4.8. Excitation spectrum of ethylene.

The energies and intensities of the most important peaks and shoulders of the spectra are combined in Tables 4.4 and 4.6.
The low energy peaks in the 1 – 2.5 eV region are ascribed to the formation of transient negative ions. The intensity and to a certain extent the energy of the peaks depend on the well depth used. However, a lower limit for the electron affinities of the molecules can be derived from the data. For example for ethylene and cis-butene-2 the electron affinities (A) will be > -1.8 and > -2.3 eV respectively. These data should probably not be compared with results obtained from the measurements of the equilibrium between the molecule and the negative ion. It is likely that the present data refer to vertical electron affinities. Consequently they can be compared with calculations where the same configuration of the molecule is assumed for the ground and the negative ion state.
Hush and Pople (1955) predicted $A = -1.81$ eV while Hoyland and Goodman (1962) found $A = -1.69$ for the ethylene molecule. Both values are in surprisingly good agreement with the experimental value $A > -1.8$ eV (Table 4.6).

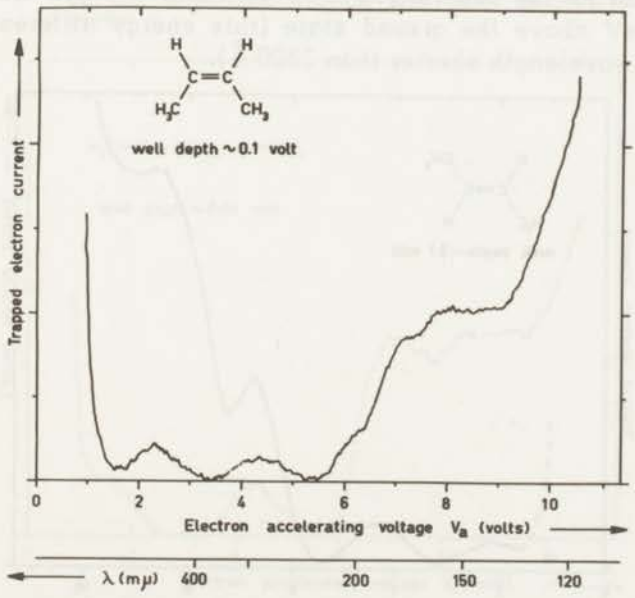

Fig. 4.9. Excitation spectrum of cis-butene-2.

In all olefins a triplet band shows up near 4 eV which is probably due to a $\pi \rightarrow \pi^*$ transition. In ethylene this band extends from about 3.4 eV (3700 Å) up to 5.7 eV (2200 Å).

For cis-butene-2 and tetramethylethylene a definite shoulder (the olefin mystery band) appears near 6 eV. The difference between the spectra for these compounds and those for the other olefins can be explained by assuming that the repulsion between the methyl groups gives rise to a perturbation of the symmetry of the molecule. This would enhance the intensity of a symmetry forbidden transition. It is also possible that for some molecules the mystery band remains hidden under the strong band near 7 eV.

The result presented in this thesis for the saturated hydrocarbons indicate that besides the low energy singlet - singlet and singlet - triplet transitions of the $\pi \rightarrow \pi^*$ or $\sigma \rightarrow \pi^*$ type one may expect at somewhat higher excitation energies, starting at about 6 eV (2100 A), singlet - triplet transitions of the $\sigma \rightarrow \sigma^*$ type.
This indicates that in this type of molecules the applicability of the usual σ —— π separability (see for example Lykos and Parr, 1956) is very doubtful for the calculation of excited states which are more than about 5.5 eV above the ground state (this energy difference corresponds to a wavelength shorter than 2300 Å).

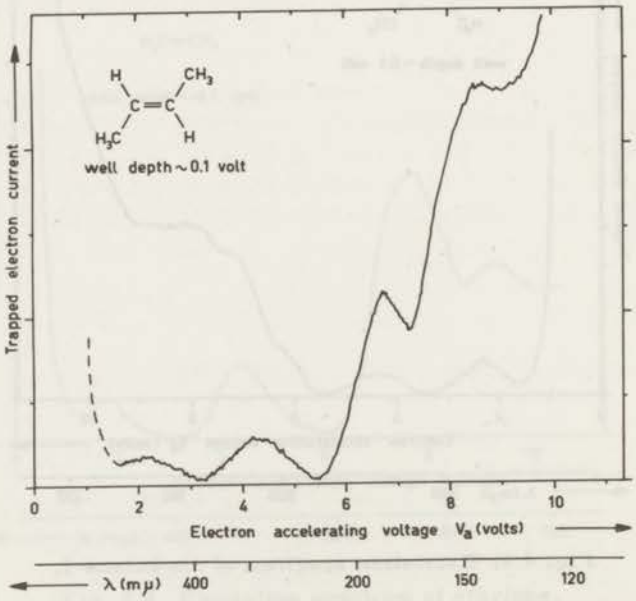

Fig. 4.10. Excitation spectrum of trans-butene-2.

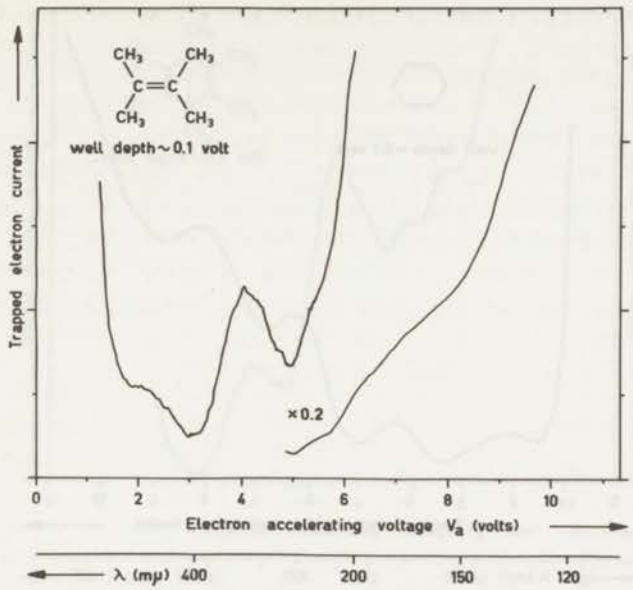

Fig. 4.11. Excitation spectrum of 2,3-dimethylbutene-2. For the right hand side of the spectrum the sensitivity of the detection system has been decreased by a factor 5.

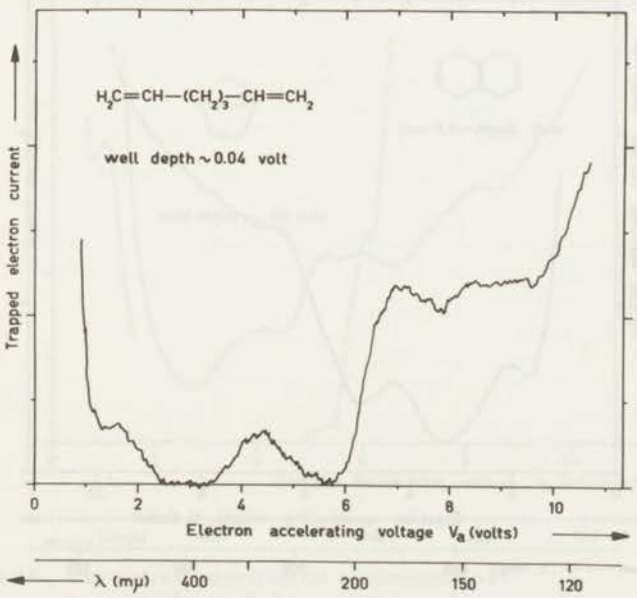

Fig. 4.12. Excitation spectrum of 1,6-heptadiene.

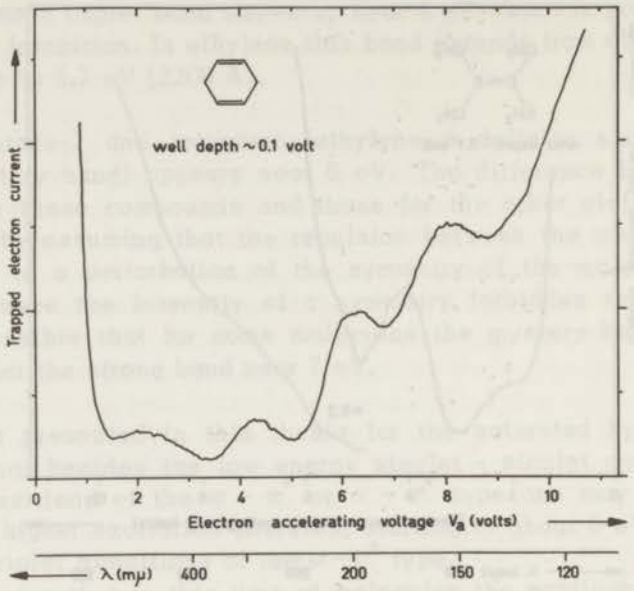

Fig. 4.13. Excitation spectrum of 1,4-cyclohexadiene.

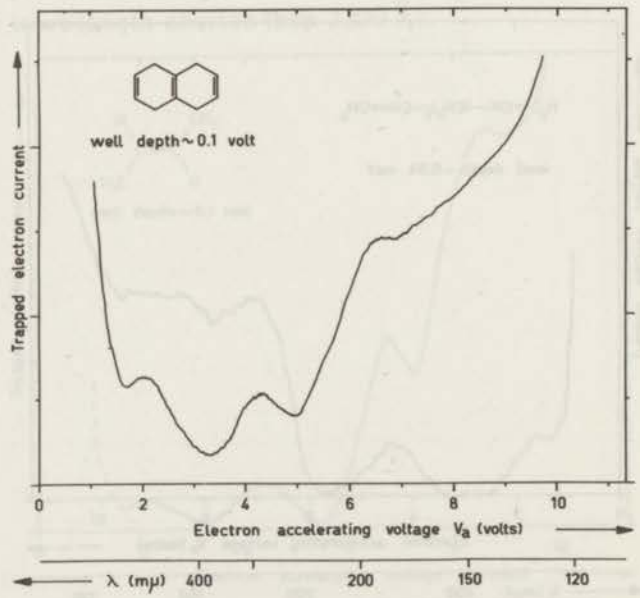

Fig. 4.14. Excitation spectrum of isotetraline.

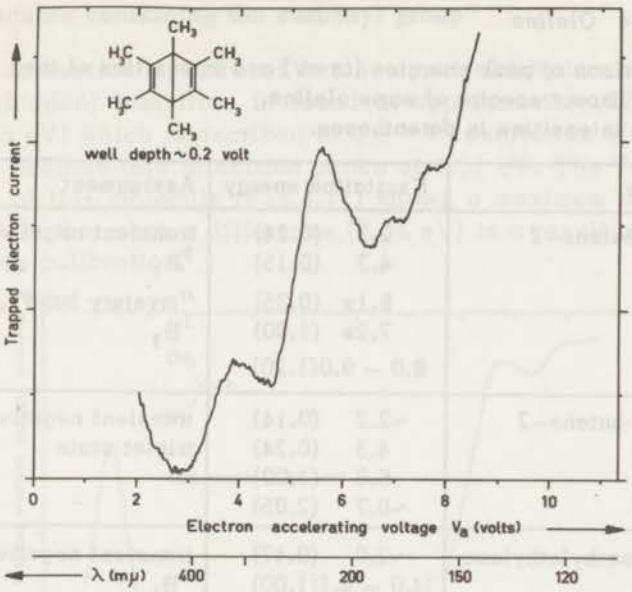

Fig. 4.15. Excitation spectrum of hexamethylbicyclo [2,2,0] hexa-2,5-diene (hexamethyl-Dewar-benzene).

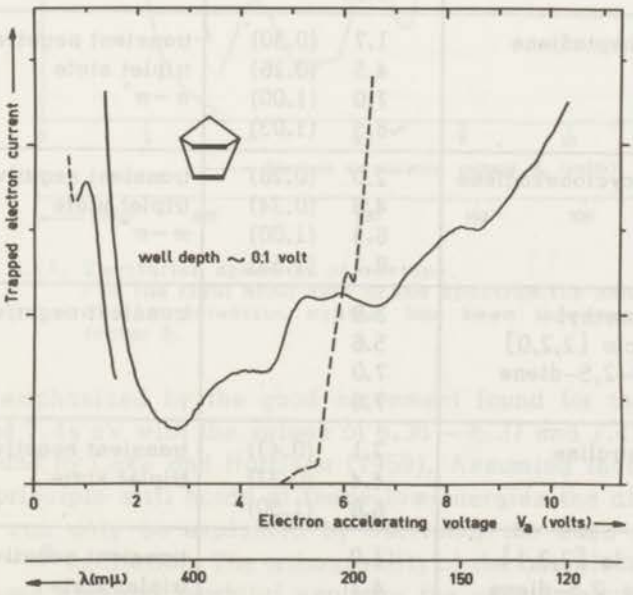

Fig. 4.16. Excitation spectrum of norbornadiene (bicyclo [2,2,1] hepta-2,5-diene)
------ optical excitation spectrum (solution in cyclohexane).

Table 4.4 *Olefins*

A comparison of peak energies (in eV) and intensities of the electron impact spectra of some olefins.
Relative intensities in parentheses.

Molecule	Excitation energy	Assignment
1. cis–butene–2	2.3 (0.24) 4.3 (0.15) 6.1s (0.35) 7.2s (1.00) 8.0 – 9.0(1.20)	transient negative ions $^3B_1$ "mystery band", $\pi \rightarrow \sigma^*$ $^1B_1$
2. trans-butene–2	~2.2 (0.14) 4.3 (0.24) 6.8 (1.00) ~8.7 (2.05)	transient negative ions triplet state
3. tetramethylethylene	~2.0 (0.47) 4.0 – 4.1(1.00) 5.7s 8.3s	transient negative ions $^3B_{1u}$ "mystery band", $\pi \rightarrow \sigma^*$
4. 1,6–heptadiene	1.7 (0.30) 4.5 (0.26) 7.0 (1.00) ~8.5 (1.03)	transient negative ions triplet state $\pi \rightarrow \pi^*$
5. 1,4–cyclohexadiene	2.0 (0.28) 4.3 (0.34) 6.3 (1.00) 8.1 (1.55)	transient negative ions triplet state $\pi \rightarrow \pi^*$
6. hexamethyl bicyclo [2,2,0] hexa–2,5–diene	3.9 5.6 7.0 7.6	transient negative ions
7. isotetraline	2.1 (0.43) 4.4 (0.37) 6.6 (1.00)	transient negative ions triplet state
8. bicyclo [2,2,1] hepta–2,5–diene (norbornadiene)	1.0 4.1 5.3 5.9 8.3	transient negative ions triplet state

4.6. Molecules containing the carbonyl group

In light absorption spectra of ketones and aldehydes a weak (symmetry forbidden) transition is found at approximately 270 – 330 mμ (3.8 – 4.6 eV) which is ascribed to a $n \rightarrow \pi^*$ excitation of the carbonyl group. In acetone this transition peaks at 4.51 eV. The TE excitation spectrum of this molecule (Fig.4.17) shows a maximum at 4.1^5 eV. It is not likely that such a difference (0.35 eV) is a result of an inaccurate energy calibration.

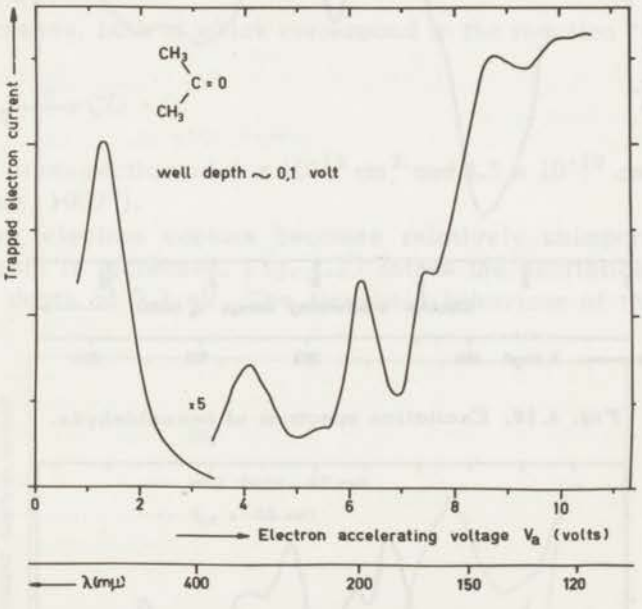

Fig. 4.17. Excitation spectrum of acetone.
For the right hand side of the spectrum the sensitivity of the detection system has been increased by a factor 5.

This is emphasized by the good agreement found for the transitions at 6.3 and 7.45 eV with the values of 6.36 – 6.37 and 7.45 eV respectively found by Lake and Harrison (1959). Assuming that the Franck-Condon principle still holds at these low-energies the discrepancy of 0.35 eV can only be explained by ascribing the band to a vertical triplet $n \rightarrow \pi^*$ excitation. The orthogonality of the one electron n-orbital and the one electron π-orbital explains the very small singlet-triplet splitting for such a transition. Experimentally a 0.4 eV separation is found in the case of formaldehyde (Henderson and Muramoto, 1965; Hodges, Henderson and Coon, 1958).

The similarity between the spectra of benzaldehyde and acetophenone (Fig.4.18, Fig.4.19) is obvious. It is difficult to decide whether the

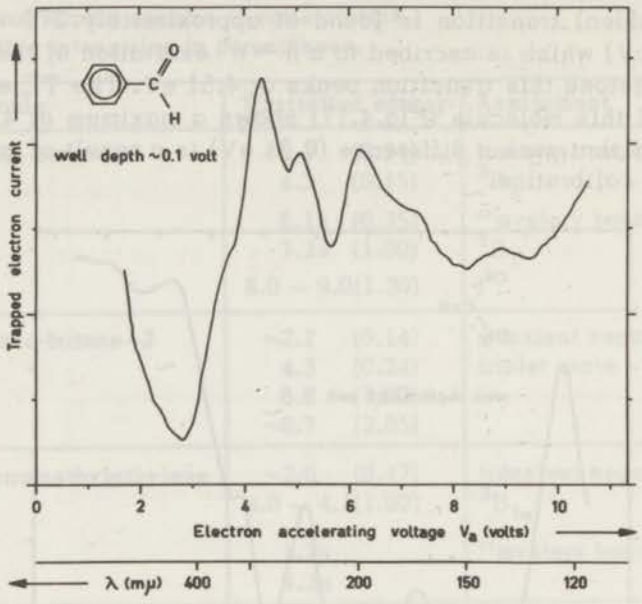

Fig. 4.18. Excitation spectrum of benzaldehyde.

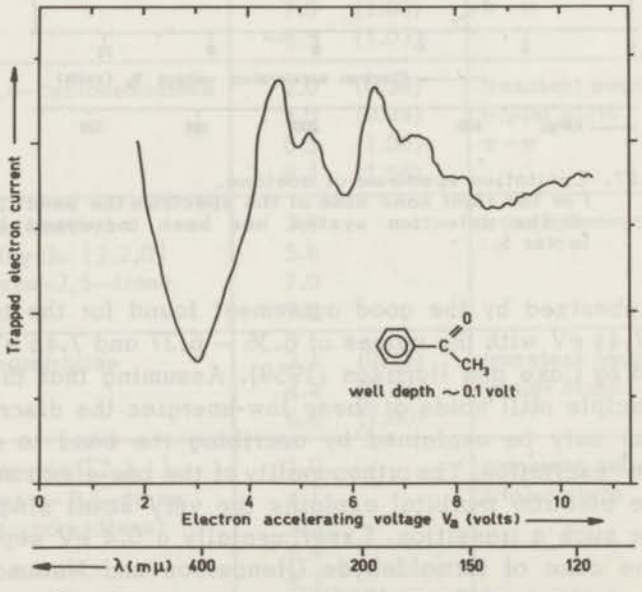

Fig. 4.19. Excitation spectrum of acetophenone.

shoulder at 3.8 eV in benzaldehyde and at 4.0 eV in acetophenone results from the singlet or triplet $n \rightarrow \pi^*$ transition. A striking feature of both spectra is the intense band at about 4.5 eV. In table 4.5 the excitation energies and relative intensities are presented together with comparable data from other sources.

For carbon dioxide the excitation spectrum is very much dependent on the well depth, the formation of negative ions being observed for even a zero trapping potential. The positions of the maxima in the cross section for dissociative electron-capture are approximately at 4.4 and 8.2 eV.

These processes, both of which correspond to the reaction

$$CO_2 \xrightarrow{e} CO + O^-$$

have small cross sections: 1.5×10^{-19} cm^2 and 4.5×10^{-19} cm^2 respectively (Schulz, 1962[b]).

Dissociative electron capture becomes relatively unimportant when the well depth is increased. Fig. 4.20 shows the excitation spectrum for a well depth of 0.2 eV. The threshold behaviour of the process

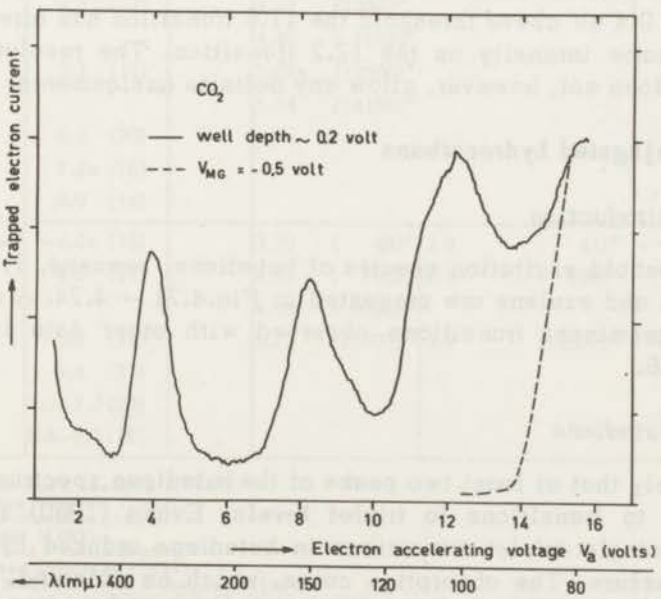

Fig. 4.20. Excitation spectrum of carbon dioxide for a well depth of 0.2 volt. The production of positive ions is shown in broken lines.

near 4 eV (Fig.5.6) is similar to that for nitrogen at 2eV. This suggests that the formation of transient negative ions is involved. Such an interpretation is in agreement with the observed shift of the position of the maximum as a function of the well depth. It is probable that the two processes near 4 eV have the same origin

$$CO_2 \xrightarrow{\text{electron impact}} CO_2^- \begin{cases} \rightarrow CO + O^- + \text{kinetic energy} \\ \rightarrow CO_2 + e + \text{vibrational energy} \end{cases}$$

where the dissociation can only occur for the higher vibrational levels (maximum at 4.4 eV).
The shoulder at 2 eV can be interpretated as due to the direct vibrational excitation of CO_2.

A strong dependence on the well depth is also observed for the excitation function in the region 7 – 10 eV and 11 – 13 eV. Near threshold peaks are observed at 8.3 and 12.2 eV but with increasing well depth the importance of transitions at 9.0 and 11.6 eV becomes appreciable. At about 0.4 eV above threshold the 11.6 transition has already attained the same intensity as the 12.2 transition. The resolution of the spectra does not, however, allow any definite assignments.

4.7. Conjugated hydrocarbons

4.7.1. Introduction

The threshold excitation spectra of butadiene, benzene, 1,1-diphenylethylene and azulene are presented in Fig.4.21 – 4.24. A comparison of the prominent transitions observed with other data is given in Table 4.6.

4.7.2. Butadiene

It is likely that at least two peaks of the butadiene spectrum (Fig.4.20) are due to transitions to triplet levels. Evans (1960) has studied optical singlet-triplet transitions in butadiene induced by oxygen at high pressure. The absorption curve, which he obtained, shows two maxima the first at 3.2 eV and the second at 3.9 eV. The transitions are identified as leading to the first and second triplet state. In our spectrum there is a diffuse band in this region with a very vague shoulder at 3.3 eV and a broad peak at 3.8 eV. A weak transition is

Table 4.5 *Molecules containing the carbonyl group.*
A comparison of peak energies (in eV) and intensities of this research with other data.
Relative intensities are in parentheses.

Molecule	Electron impact		Light absorption		Assignment
	this research	other authors			
acetone	1.3 (20)				transient negative ions
	4.1[5] (7)				triplet n $\rightarrow \pi^*$
		~4.3[a]	4.5 (15)[b]		singlet n $\rightarrow \pi^*$
	6.2[5] (12)	~6.4[a]	6.3 (6400)[b]	6.36–6.37 (9120)[c]	
				6.50–6.50[5] (6610)[c]	
				6.64 (1950)[c]	
	7.4[5] (13)			7.45 (1620)[c]	
			8.1 (11000)[b]		
	8.7[5] (25)		8.8–8.9 (9800)[b]		
	~10.0 (26)				
benzaldehyde	3.8s (14)		3.12[d]; 3.34[d]; 3.50[d]; 3.66[d]; 3.82[d]		n $\rightarrow \pi^*$[h]
	4.3 (24)		4.32 (1000)[e]		
			4.46 (1150)[e]		
	5.1 (19)		5.02s (11500)[e]		
			5.14 (14100)[e]		
	6.2 (20)				
	7.2s (16)				
	8.9 (14)				
acetophenone	~4.0s (15)		3.70 (49)[f]	3.9 (41)[g]	n $\rightarrow \pi^*$
	4.6 (24)		4.33 (790)[f]	4.5 (890)[g]	
			4.48 (1000)[f]		
	5.2 (21)		5.23 (12900)[f]	5.2 (12600)[g]	
	6.4 (23)				
	7.2–7.3 (20)				
	8.0–8.2 (18)				

a. Silverman and Lassettre (1965[b]).
b. Barnes and Simpson (1963).
c. Lake and Harrison (1959).
d. Stockburger (1962).
e. Dearden and Forbes (1958).
f. Lutskii and Dorofeev (1957).
g. Tanaka, Nagakura and Kobayashi (1956).
h. The very weak transition at 3.12 eV is identified as the 0 – 0 transition of the triplet n $\rightarrow \pi^*$. The other bands are due to the much more intense singlet excitation. The overlap with these transitions did not permit the detection of higher vibrational levels of the triplet state.

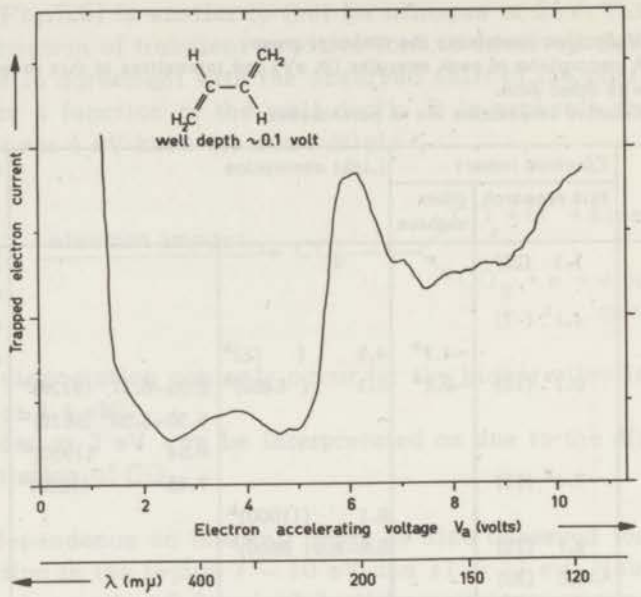

Fig. 4.21. Excitation spectrum of butadiene.

observed at 4.8 eV which may also be due to a singlet-triplet transition. This interpretation is supported by the good agreement of our peak values at 3.8 and 4.8 eV with calculations of Pariser and Parr (1953). Their values of the two lowest triplet levels are 3.9 and 4.6 eV.

4.7.3. *Benzene*

The threshold excitation spectrum of benzene is presented in Fig. 4.22. The transition to the $^1E_{1_u}$ state at 6.9 eV, which is symmetry allowed for dipole transitions, is the most pronounced peak. The symmetry forbidden transitions at 4.7 eV and 6.0 eV are, however, also of comparable intensity. This is in contrast to UV absorption data.
Compton et al. (1967) obtained an excitation spectrum of this molecule using a different technique. Their method is based on the appearance of SF_6^- ions which are formed when the incident electrons have a kinetic energy just exceeding threshold.
In both spectra the relative intensities of the observed transitions are, with one exception, almost identical. This exception lies in the 4.2 to 5.3 eV region where Compton et al.(1967) observe a peak more than twice as high as the one in our spectrum.
This band shows a shoulder which is interpretated as a transition to

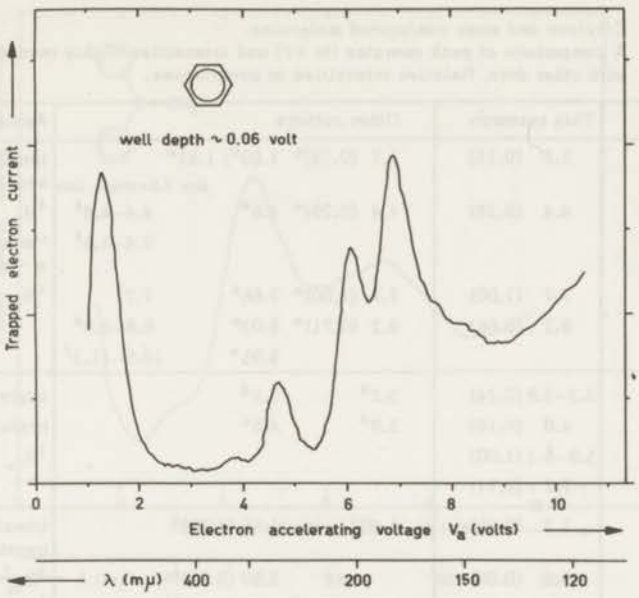

Fig. 4.22. Excitation spectrum of benzene.

the second triplet state. The reason for this discrepancy is not understood. It may be that the addition of small quantities of SF_6 and HCl, which are inherent in the method of Compton et al. is responsible for the difference.
The low-energy inelastic transition at ~ 1.3 eV is assigned as due to the formation of transient negative ions. The energy of the peak indicates that the vertical electron affinity $A > -1.3$ eV is in good agreement with the value $A = -1.40$ eV calculated by Hush and Pople (1955).

The good agreement between the electron impact and optical data (Table 4.6) suggests that the influence of σ-electrons is small. The absence of theoretical calculations taking into account all electrons involved, however, makes the interpretation somewhat speculative.

4.7.4. 1,1-Diphenylethylene

The threshold excitation spectrum of 1,1-diphenylethylene is displayed in Fig.4.23. The shoulder at 3.4 eV, which is not observed in UV absorption spectra, is interpreted as an excitation to a triplet state.

Table 4.6 *Ethylene and some conjugated molecules.*
A comparison of peak energies (in eV) and intensities of this research with other data. Relative intensities in parentheses.

Molecule	This research	Other authors	Assignment
ethylene	1.8 (0.15)	1.7 (0.19)[a] 1.69[b]; 1.81[c]	transient negative ions
	4.4 (0.28)	4.4 (0.29)[a] 4.6[d] 4.4–4.8[f]	$^3B_{1u}$
		6.4–6.6[f]	"mystery band" $\pi \rightarrow \sigma^*$
	7.7 (1.00)	7.7 (1.00)[a] 7.66[e] 7.7[f]	$^1B_{1u}$
	9.2 (0.66)	9.2 (0.71)[a] 9.03[e] 8.8–9.0[f]	
		9.95[e] 10.5–11.3[f]	
butadiene	3.3–3.8 (0.24)	3.2[d] 3.9[g]	triplet state
	4.8 (0.18)	3.9[d] 4.6[g]	triplet state
	5.8–6.1 (1.00)		$^1B_{1u}$
	7.1 (0.71)		
benzene	1.3 (0.95)	1.40[c] 1.55 (1.30)[i]	transient negative ions
	3.9 (0.08)	3.90 (0.05)[i]	$^3B_{1u}$
	4.7 (0.31)	4.9 (0.004)[h] 4.80 (0.71)[i]	$^1B_{2u}$, $^3B_{2u}$, $^3E_{1u}$
	6.0 (0.72)	6.1 (0.13)[h] 6.16 (0.71)[i]	$^1B_{1u}$
	6.9 (1.00)	6.7 (1.00)[h] 6.96 (1.00)[i]	$^1E_{1u}$
1,1–ethylene	3.4 (0.36)		triplet state
	4.5 (1.00)		
		5.0 (0.26)[h]	
		5.4 (0.37)[h]	
		6.0 (1.00)[h]	
	7.2 (0.68)		
pyridine	~4.2[s]	4.31[j]	$n \rightarrow \pi^*$
	4.9 (0.62)	4.84 (1900)[h] 4.75[j]	$n \rightarrow \pi^*$
		4.93 (2000)[h]	
	5.3[s] (0.57)		
		6.16 (4850)[h]	
	6.3 (0.88)	6.27 (6000)[h]	
		6.37 (6000)[h]	
	7.2 (1.00)		
	8.3 (0.82)		
	~8.9 (0.74)		

a. Low-energy electron impact values (Bowman and Miller, 1965).
b. Theoretical values (Hoyland and Goodman, 1962).
c. Theoretical values (Hush and Pople, 1955).
d. Optical values (Evans, 1960).
e. Electron impact values. (Lassettre and Francis, 1964).
f. Low-energy electron impact values (Kuppermann and Raff, 1963[a]).
g. Theoretical values (Pariser and Parr, 1953).
h. Optical values for a solution in n–hexane (UV Atlas, 1966).
i. Low-energy electron impact values (Compton et al., 1967).
j. Optical values (Rush and Sponer (1952).

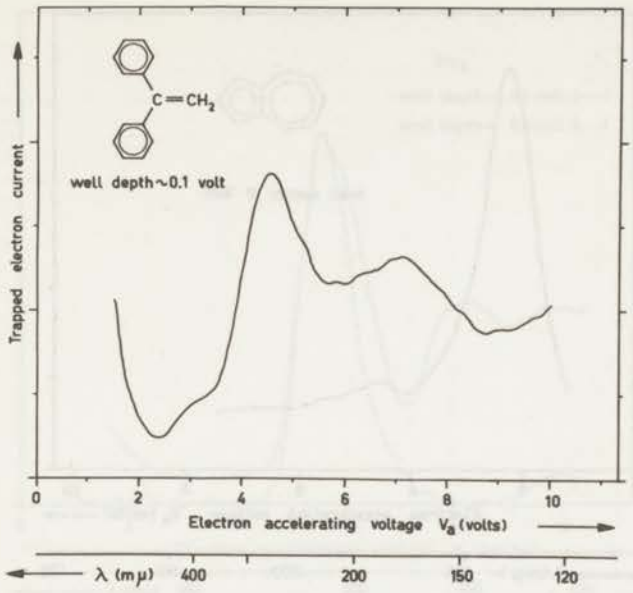

Fig. 4.23. Excitation spectrum of 1,1-diphenylethylene.

4.7.5. *Azulene*

Efforts to obtain an excitation spectrum of azulene were unsuccessful. This is due to the large cross section for dissociative electron capture(section 4.9). A spectrum showing the production of negative ions as a function of the incident electron energy is presented in Fig.4.24.

4.8. Molecules containing a nitrogen atom

The trapped electron spectra of pyridine, ammonia, triethylamine and quinuclidine are shown in Fig.4.25 – 4.28. For pyridine the peak values and intensities are compared with optical data in Table 4.6. The relatively high intensities of $n \rightarrow \pi^*$ transitions is evident. Probably, as was the case for the $n \rightarrow \pi^*$ transitions in aldehydes and ketones (section 4.6) the energy difference between the singlet-triplet and the singlet-singlet transition will be very small. At present it is not possible to decide which of these transitions is most important.

For ammonia dissociative electron capture (section 4.9) is observed besides electronic excitation (Fig.4.26).

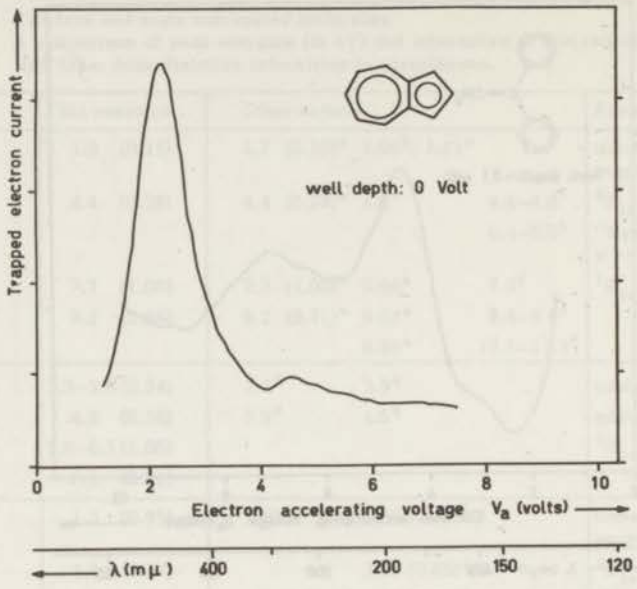

Fig. 4.24. Formation of negative ions from azulene.

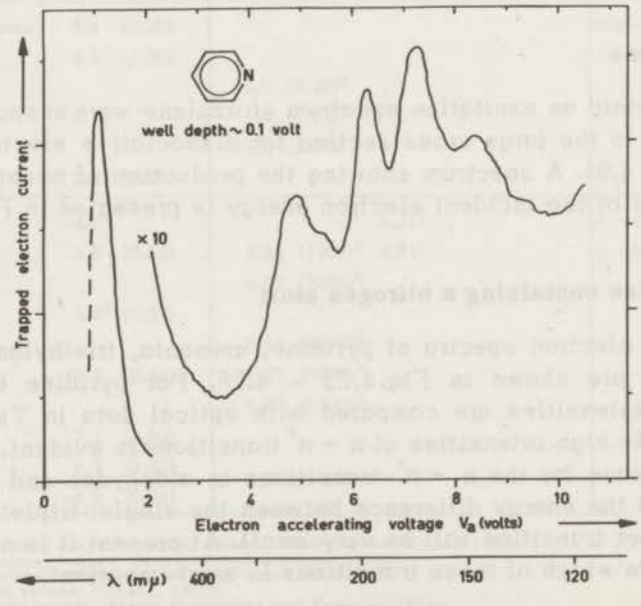

Fig. 4.25. Excitation spectrum of pyridine.
For the right hand side of the spectrum the sensitivity of the detection system has been increased by a factor 10.

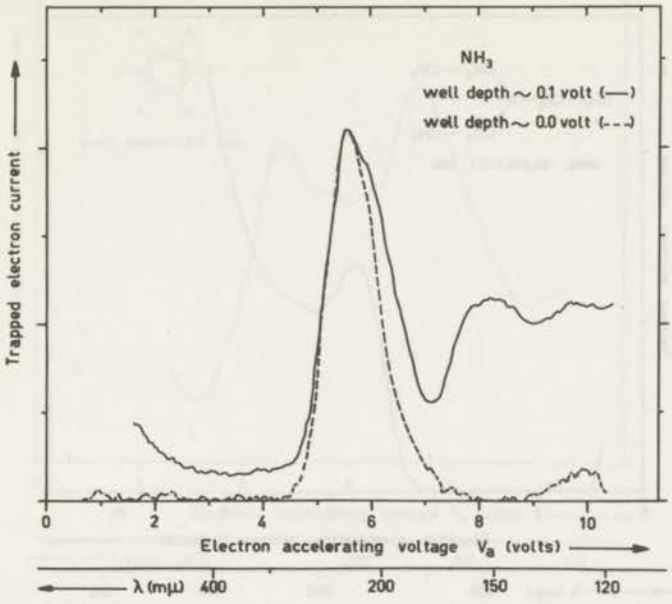

Fig. 4.26. Ammonia.
For a zero well depth only the formation of negative ions is observed, while for the well depth of 0.1 volt both electronic excitation and dissociative electron capture are involved.
The curves have been arbitrarily normalized for the peak value.

4.9. Molecules which dissociate upon electron capture

The interaction of an electron with a molecule XY may lead to the formation of a negative ion. This process can be either nondissociative or dissociative

$$e + XY \rightarrow XY^-$$

$$e + XY \rightarrow X + Y^-$$

X,Y: parts of a molecule (in general not atoms).
The first process is observed for molecules having a very small positive or a negative electron affinity for example nitrogen, carbon monoxide, carbon dioxide, ethylene, benzene, sulfurhexafluoride, etc.
Dissociative electron capture has been observed for hydrogen, oxygen, carbon monoxide (Fig.4,4), carbon dioxide, ammonia (Fig.4.26), water,

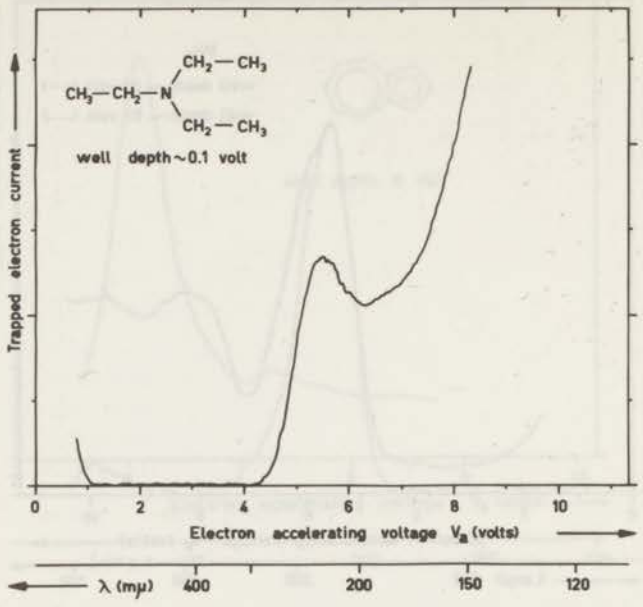

Fig. 4.27. Excitation spectrum of triethylamine.

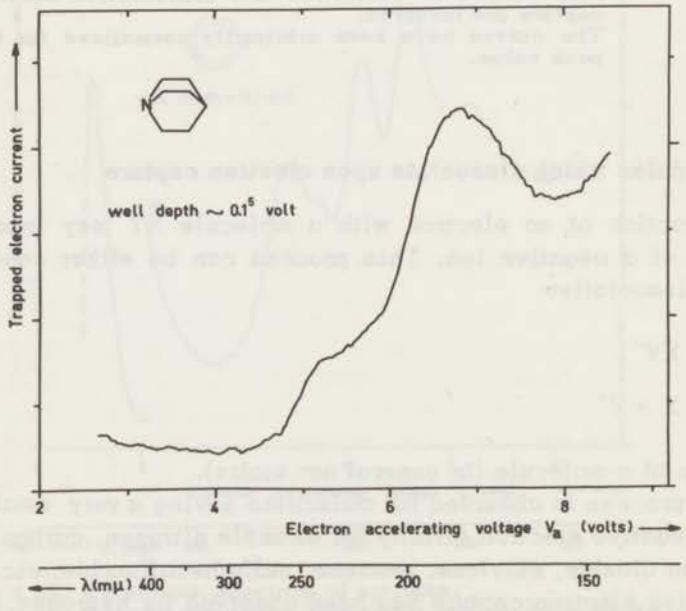

Fig. 4.28. Excitation spectrum of quinuclidine.

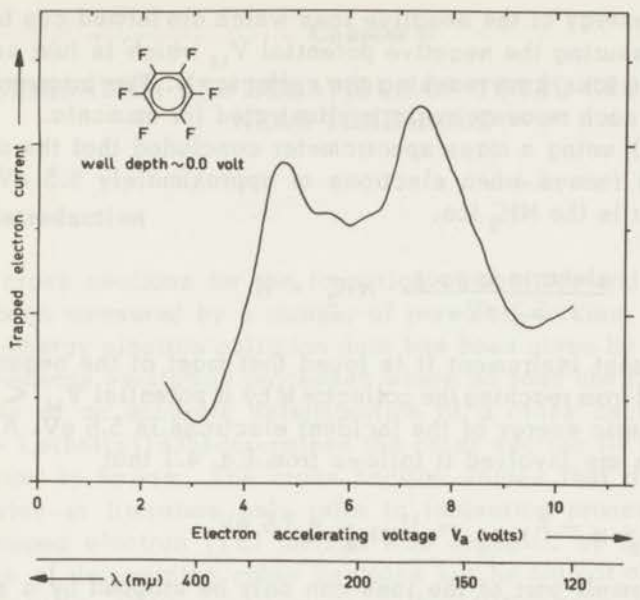

Fig. 4.29. Production of negative ions from hexafluorbenzene.

sulfurhexafluoride, azulene (Fig.4.24), nitrobenzene and hexafluorobenzene (Fig.4.29).

In the case of the first five molecules spectra have been obtained for both electronic excitation and dissociative electron capture. For the other molecules the dissociative electron capture is the predominant process near threshold. Using the laws for the conservation of energy and momentum it is possible to calculate the kinetic energy of the dissociation products.

$$E_a - D_{X-Y} + A_Y - U_X - U_{Y^-} = \frac{M_{XY}}{M_X} E_{Y^-} = \frac{M_{XY}}{M_{Y^-}} E_X \qquad (4.1)$$

E_a = kinetic energy of the incident electron.

D_{X-Y} = dissociation energy of the XY molecule.

A_Y = electron affinity of Y.

M_X, M_{Y^-}, M_{XY} = mass of the species X, Y^- and XY respectively.

E_X, E_{Y^-} = kinetic energy of the products X and Y^-.

U_X, U_{Y^-} = extra internal energy of X and Y^- when they are formed in an excited state. This can be an electronically, vibrationally or rotationally excited state.

The kinetic energy of the negative ions which are formed can be determined by measuring the negative potential V_M which is just sufficient to prevent the ions from reaching the collector M. The information one can get from such measurements is illustrated for ammonia.
Kraus (1961) using a mass spectrometer concluded that the principal ion which is formed when electrons of approximately 5.5 eV collide with ammonia is the NH_2^- ion.

$$NH_3 \xrightarrow[5.5\ eV]{\text{electron impact}} NH_2^- + H$$

With the present instrument it is found that most of the negative ions are prevented from reaching the collector M by a potential $V_M < -0.12$ V when the kinetic energy of the incident electrons is 5.6 eV. Assuming that NH_2^- ions are involved it follows from Eq. 4.1 that

$$D_{NH_2-H} - A_{NH_2} - U_{NH_2^-} = 3.6\ eV \qquad (4.2)$$

However, a small part of the ions can only be stopped by a potential $V_M < -1.8$ V.
There are, therefore, some negative ions having considerable kinetic energy. Using reasonable values of D and A, equation (4.1) can only be satisfied if ions with a very small mass are involved. These must be H^-.
Substituting the values $E_\alpha = 5.6$ eV and $E_{H^-} = 1.8$ eV in formula (4.1) it follows that

$$D_{NH_2-H} - A_H - U_{NH_2} = 3.7\ eV \qquad (4.3)$$

Using the experimentally determined value for the electron affinity of the hydrogen atom ($A_H = 0.75$ eV; Henrich, 1944) one can solve the equations (4.2) and (4.3). It follows that

$$D_{NH_2-H} < 4.4\ eV$$

$$A_{NH_2} > 0.8\ eV$$

where the equalities are reached when NH_2 and NH_2^- are formed in their ground states. The value for the dissociation of NH_3 into NH_2 and H presented by Herzberg (1966) $D_{NH_2-H} = 4.38$ eV suggests that this is the case for the NH_2 radical.

Chapter 5

DETERMINATION AND BEHAVIOUR OF TOTAL CROSS SECTIONS NEAR THRESHOLD

5.1. Introduction

Total cross sections for the formation of positive and negative ions have been measured by a number of research-workers. A compilation of low-energy electron collision data has been given by Kieffer (1967). In low-energy excitation processes where no ions are formed only one example of an accurate determination of a cross section is known. Maier - Leibnitz (1935) determined the cross section for the $1^1S \rightarrow 2^3S$ transition in helium. The cross section values that are reported for molecules in literature only refer to ionisation processes. Actually the trapped electron (TE) method was designed by Schulz with the purpose of determining cross sections but he did not obtain unambiguous results. With our apparatus the difficulties encountered by Schulz could be surmounted.

Already more than 35 years ago Smith (1930), and Tate and Smith (1932) carried out their careful experiments which up to 1965 have been used as a standard for the normalisation of cross sections. Recently accurate data for the low-energy region have been obtained by Schulz (1962^b), Asundi (1963), Rapp and Briglia (1965), and Rapp and Englander-Golden (1965). Compton (1966, 1967), Christophorou (1967) and co-workers have determined many total cross sections for the dissociative electron capture of large molecules.

In contrast to the ionisation experiments very little is known about the magnitude and behaviour of excitation cross sections near threshold. Maier-Leibnitz (1935) has determined the maximum of the cross sections for the 2^3S excitation of helium which is reached at approximately half a volt above threshold. Ever since this value has been used for the normalisation of cross sections near threshold. The reason why no other accurate data are available probably finds its origin in the difficulties encountered in the detection of excited atoms and molecules. Methods which can be used for this detection depend on the determination of

1. The intensity of fluorescence or phosphorescence light.
2. The light absorption of excited molecules (Woudenberg and Milatz, 1941).

3. The release of electrons from a metal by impinging metastables (Dorrestein, 1942; Schulz and Fox, 1957).
4. The low-energy electrons produced by an inelastic collision (indirect method).

Method 1 and 2 require a high sensitivity of the optical part of the apparatus especially when the threshold behaviour of cross sections with well defined electron beams is studied. The first method is especially difficult for molecules which can easily undergo an internal conversion to the ground state (without any light emission). The trapped electron spectra presented in this thesis are an example of the fourth method which does not suffer from any of these defects. For any inelastic process where low-energy electrons are formed the cross section can be measured.

Absolute total cross sections for processes in helium, carbon monoxide, nitrogen, oxygen, carbon dioxide, ethylene and benzene are given in Table 5.1. The results are believed to be accurate within 30%. In Figs. 5.1 – 5.8 the threshold behaviour of some transitions is shown. Unlike the excitation spectra nowhere a correction for contact potentials has been made in the spectra representing the threshold behaviour of a transition. In chapter 2 it has already been pointed out how these curves can greatly facilitate the determination of a good theoretical description of the collision process involved.

5.2. Experimental procedures

The trapped electron (TE) method can be employed to study the threshold behaviour of transitions. The simplest method (method 1) consists of recording a TE spectrum for a large well depth, for instance 2 volts. In section 3.4.2 it has been outlined that for each excitation process the cross section is now plotted up to an energy of 2 volts above threshold. A similar result can be obtained (method 2) by plotting the trapped electron current for a constant accelerating voltage as a function of a varying well depth. The well depth is calculated from the potential V_{MG} of the trapped electron collector M with respect to the collision chamber. In those cases where both methods can be used a comparison of the results makes it possible to check the correctness of the calculation of the well depth. The applied accelerating voltage V_a is chosen in such a way that eV_a equals the excitation energy eV_e of the state under investigation. By consequence (formula 3.5 and 3.6) a spectrum is obtained for the total cross section as a function of the energy ΔE of the trapped electrons. For this type of

spectrum the resolution is very good near threshold but decreases with increasing well depth.

Both methods have been applied to the $1\,^1S \rightarrow 2\,^3S$ transition in helium. In Fig. 5.1 it is shown that assuming $\Delta E = 0.17$ eV$_{MG}$ a good agreement is observed between the methods. This confirms the determinations of the well depth presented in chapter 3. The cross section for the first maximum in the curve which is reached at about half a volt above threshold is, as it should be, within experimental error independent of the well depth being used for the determination. This is a significant improvement with regard to the behaviour of the apparatus

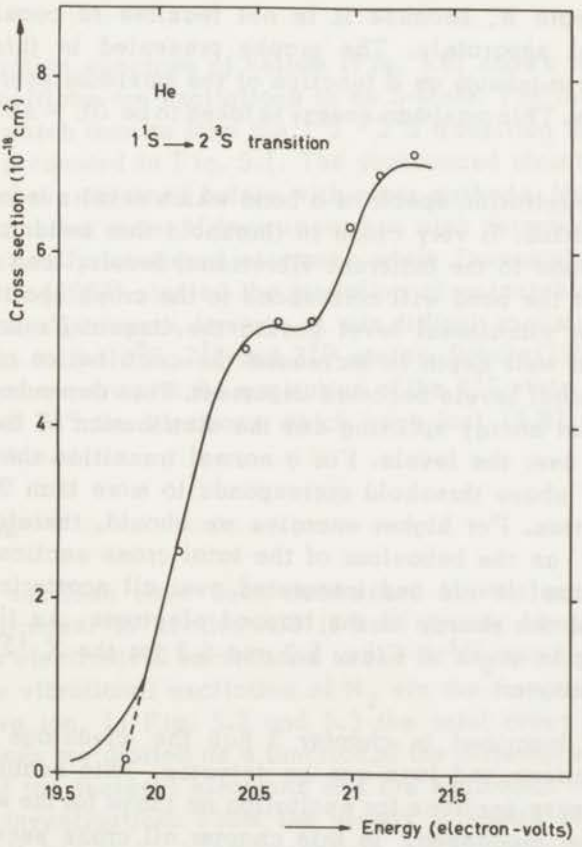

Fig. 5.1. The threshold behaviour of the cross section for the $1\,^1S \rightarrow 2\,^3S$ transition in helium is determined by two different methods (see section 5.2).
—— constant well depth of 2 volts.
o o o variable well depth.

of Schulz (1958) where changes in the cross section were observed which amounted to more than 50%. Such deviations may result from an inefficient discrimination between the high-energy (especially the elastically scattered and the low-energy electrons because this energy selection becomes less effective for increasing well depths (section 3.4.1). The effect may also result from a slight defocussing of the electron beam due to the applied potential V_{MG}. These problems can be remedied by increasing the strength of the magnetic field.

With molecules only the second method can be used. The maximum intensity of a whole band is determined for increasing values of the average well depth W, because it is not feasible to consider each vibrational level separately. The graphs presented in this chapter are plots of this maximum as a function of the maximum energy of the trapped electrons. This maximum energy is taken to be $\Delta E = eW = 0.16\, V_{MG}$ (section 3.4.2.).

Consider in an excitation spectrum a band which results from a single electronic transition. If very close to threshold this band is resolved into the transitions to the different vibrational levels, then the maximum intensity of the band will correspond to the cross section for the transition to the vibrational level having the largest Franck-Condon factor. When the well depth is increased the contribution of the surrounding vibrational levels becomes important. This depends of course on the vibrational energy splitting and the distribution of the Franck-Condon factors over the levels. For a normal transition the intensity at about 0.4 eV above threshold corresponds to more than 90% of the total cross section. For higher energies we should, therefore, interpret the curves as the behaviour of the total cross section (summed over all vibrational levels and integrated over all scattering angles) as a function of the energy of the trapped electrons. An illustration of the foregoing is given in Figs. 5.2 and 5.3 for the $X\ ^1\Sigma_g^+ \rightarrow B\ ^3\Pi_g$ transition in nitrogen.

The apparatus described in chapter 3 has the advantage that both low-energy electrons and ions can be detected. This enables one to normalize the cross sections for excitation on those for the well established ionisation processes. In this chapter all cross sections have been normalized on the value of Rapp and Englander-Golden (1965) for the ionisation of carbon monoxide in the 14.5 – 15.5 eV region. They found for this region

$$\frac{\Delta Q}{\Delta E} = 4.9 \times 10^{-18}\ \mathrm{cm}^2/\mathrm{eV} \qquad (5.2)$$

ΔQ = increase of the cross section Q for the ionisation.
ΔE = excess energy of the incident electrons above the threshold for ionisation.

Assuming this value we find for the maximum of the cross section for the 2^3S excitation of helium: $5.2 \times 10^{-18} cm^2$ which is in excellent agreement with the value $5 \times 10^{-18} cm^2$ of Maier-Leibnitz (1935). The maximum cross section for the formation of negative ions from O_2 near 6.5 eV is found to be $1.4 \times 10^{-18} cm^2$. Rapp and Briglia (1965) determined the same value for this process.

5.3. Helium

The TE excitation spectrum of helium (Fig. 3.6) shows that the most important transitions are excitations to an S-state. For the first peak, at 19.82 eV, which results from the $1^1S \rightarrow 2^3S$ transition the threshold behaviour is presented in Fig. 5.1. The pronounced structure which is observed has been obtained before with other methods. Maier-Leibnitz (1935) using another type of instrument has also determined the number of inelastically scattered electrons while Dorrestein (1942) and Schulz and Fox (1957) studied the formation of metastable atoms from helium. In these experiments, however, it was difficult to distinguish among the transitions to the 2^3S, 2^1S and 2^3P states. Schulz (1964[b]) obtained a well resolved spectrum for the excitation of the 2^3S state by measuring at an angle of 72° the electrons which have lost 19.82 eV in an inelastic collision.

5.4. Nitrogen

Total cross sections have been determined for the prominent transitions in nitrogen. In section 4.2 it has already been shown that these are the electronical excitations to the $B\ ^3\Pi_g$ and $E\ ^3\Sigma_g^+$ ($E\ ^1\Sigma_g^+$) state and the vibrational excitation of N_2 via the formation of a transient negative ion. In Fig. 5.2 and 5.3 the total cross sections for these processes are plotted as a function of the difference ΔE between the energy of the incident electrons and the excitation energy of the state under investigation. From the graphs it seems plausible that about 0.09 eV has to be subtracted from ΔE in order to correct for contact potentials.

In the case of the excitation to the $B\ ^3\Pi_g$ state the cross section is a linear function of ΔE. This agrees with the work of previous authors on the formation of metastable molecules; however, the present assign-

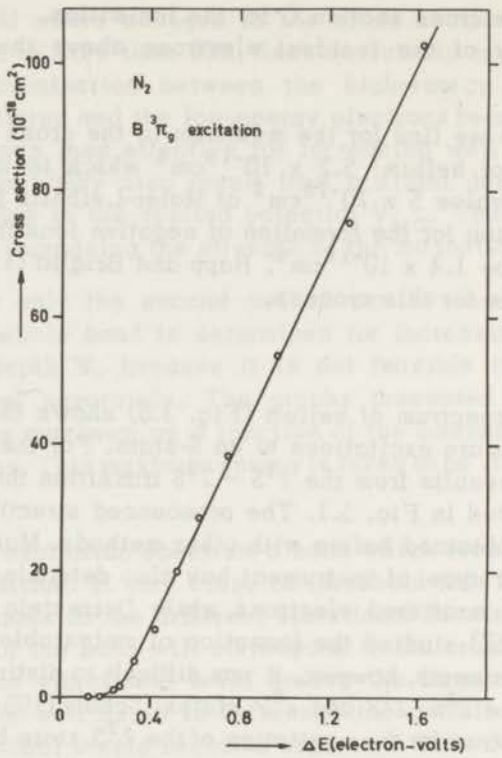

Fig. 5.2. Threshold behaviour of the cross section for the $X\ ^1\Sigma_g^+ \rightarrow B\ ^3\Pi_g$ transition in nitrogen.
No correction for contact potentials has been made.

ment of the transition is different (see section 4.2). An almost linear behaviour is also predicted by the classical theory of Bauer and Bartky (1965) but the magnitude is found to be about seven times larger in the experiment.
For the excitation of the $E\ ^{1,3}\Sigma_g^+$ state the cross section increases rapidly near threshold but seems to approach a maximum soon. An explanation for this behaviour has been given in chapter 2. The excitation process could only be followed up to about 0.4 eV above threshold because of the increasing relative importance of the excitation to near-by states.

The maximum of the cross section for the vibrational excitation near 2 eV of nitrogen increases much faster above threshold than the cross

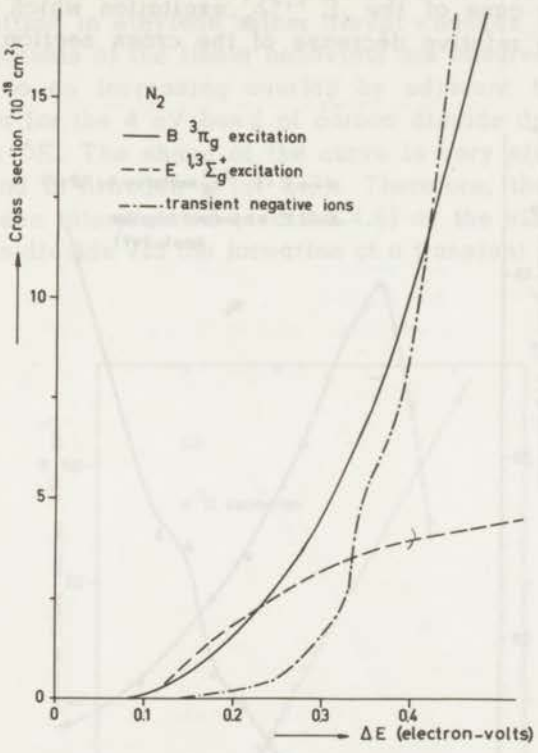

Fig. 5.3. Nitrogen (see sections 5.2 and 5.4).
For the $X\ ^1\Sigma_g^+ \rightarrow E\ ^{1,3}\Sigma_g^+$ transition the intensity has been corrected for the overlap by other electronic transitions.

section for any of the other processes. The curve shows a definite structure because the number of vibrational states which are included in a spectrum increases with the well depth (Fig. 4.2). The result in Fig. 5.3 which is obtained for the maximum of the band may also include transitions via different electronic configurations of the N_2^- ion. The vibrational energy splitting $\Delta E_v = 0.28$ eV of the N_2^- ion which was determined by Schulz (1964[a]) at 72° scattering is rather large to explain the behaviour in the present spectrum. It is quite possible, however, that the influence of other negative ion states is important for the total scattering cross section. In Fig. 5.4 the ratios of the cross sections are plotted as a function of the excess energy ΔE. For the vibrational excitation such a spectrum has the advantage that the influence of the overlap of near-by vibrational levels is largely elimin-

ated. For the case of the $E\,^{1,3}\Sigma_g^+$ excitation which is an isolated transition the relative decrease of the cross section is much exaggerated.

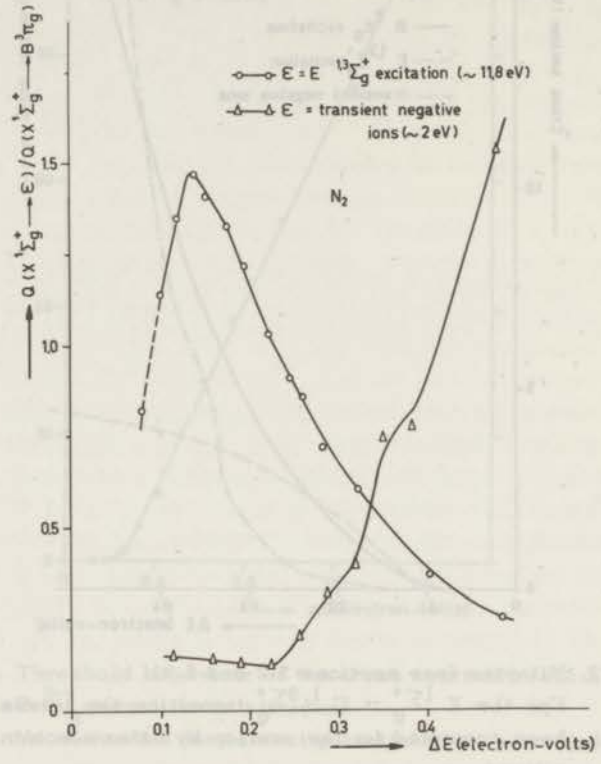

Fig. 5.4. Nitrogen (see sections 5.2 and 5.4).

5.5. Other molecules

For some of the transitions which have been discussed in chapter 4 the threshold behaviour has been determined. The results for carbon monoxide, carbon dioxide, ethylene and benzene are displayed in Fig. 5.5 – 5.8. In many cases the cross section is a linear function of the excess energy ΔE above threshold. For the case of the 8 eV and the 12 eV band of carbon dioxide the figures may be somewhat misleading because each band presumably consists of at least two different electronic transitions for which the relative magnitudes change with ΔE.

In the excitation of the a $^3\Pi$ state of carbon monoxide and the singlet $\pi \rightarrow \pi^*$ transition in ethylene rather abrupt changes appear. Also in benzene deviations of the linear behaviour are observed but these are clearly due to an increasing overlap by adjacent transitions. The cross section for the 4 eV band of carbon dioxide does not increase linearly with ΔE. The shape of the curve is very similar to that for the 2 eV band in nitrogen (Fig. 5.3). Therefore, the transition has in analogy been interpretated (section 4.6) as the vibrational excitation of carbon dioxide via the formation of a transient negative ion.

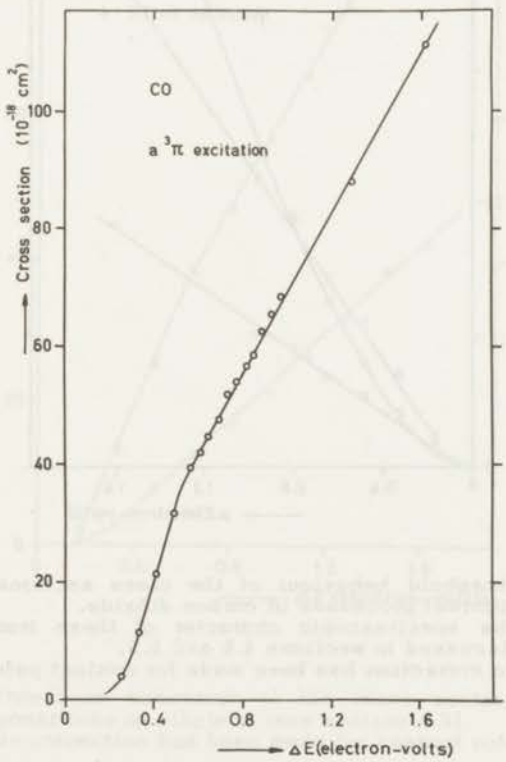

Fig. 5.5. Threshold behaviour of the cross section for the X $^1\Sigma^+ \rightarrow$ a $^3\Pi$ transition in carbon monoxide.
No correction has been made for contact potentials.

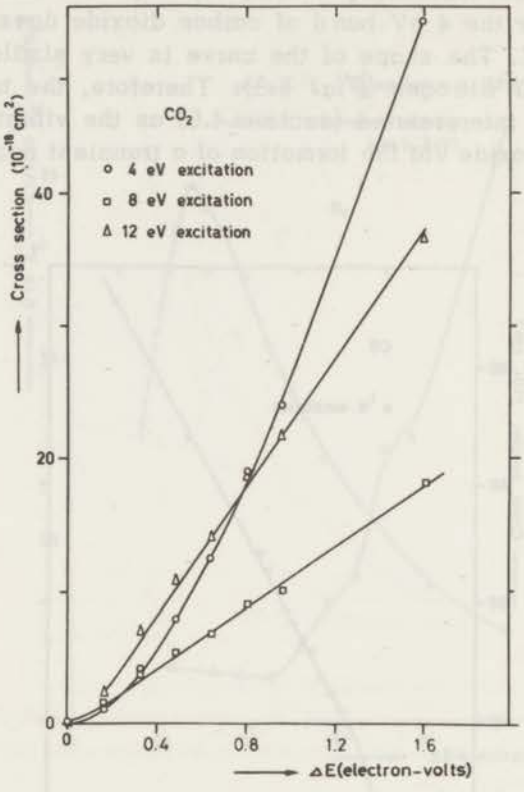

Fig. 5.6. Threshold behaviour of the cross sections for three different processes in carbon dioxide.
The spectroscopic character of these transitions is discussed in sections 4.6 and 5.5.
No correction has been made for contact potentials.

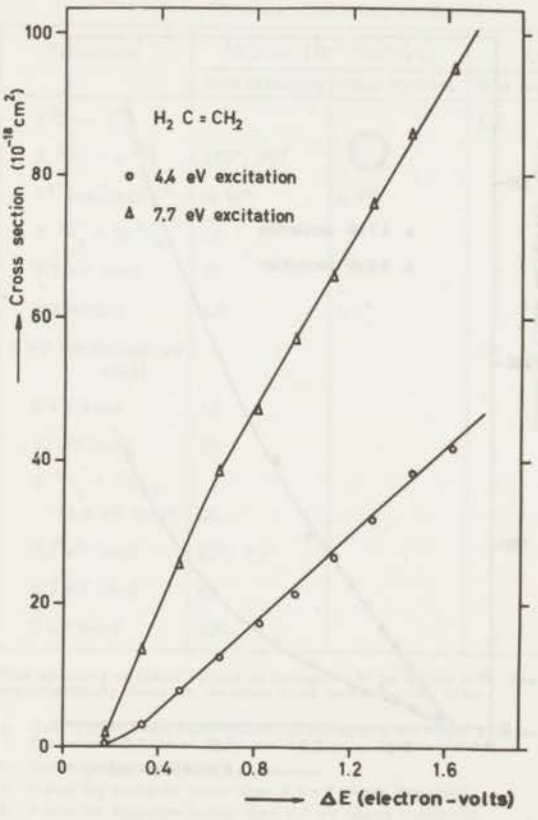

Fig. 5.7. Threshold behaviour of the cross sections for two transitions in ethylene (see section 4.5).
No correction has been made for contact potentials.

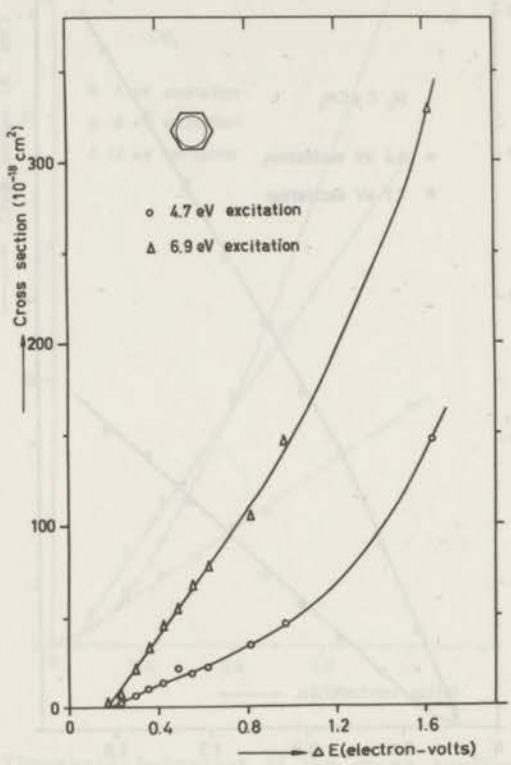

Fig. 5.8. Threshold behaviour of the cross sections of two transitions in benzene (see sections 4.7.3 and 5.5). No correction has been made for contact potentials.

Table 5.1 Absolute total cross sections.

Molecule (atom)	Transition	$\Delta Q/\Delta E$ (10^{-18}cm^2/eV)		Q_{max} (10^{-18}cm^2)	
		this research	other authors	this research	other authors
helium	$1\,^1S - 2\,^3S$			5.2	5[b]
carbon monoxide	$X\,^1\Sigma^+ \rightarrow a\,^3\Pi$	130[c]; 70[d]			
	1st ionisation[a]	(4.9)[a]	4.9[e]		
nitrogen	$X\,^1\Sigma_g^+ \rightarrow B\,^3\Pi_g$	75			
	9.5 eV band	20			
	ionisation	5.0	5.0[e]		
oxygen	5 eV band(negative ions)			1.4	1.25[f]; 1.3[gh]; 1.4[i]
carbon dioxide	8 eV band	10			
	12 eV band	25			
ethylene	$X\,^1A_g \rightarrow {}^3B_{1u}$ (4.4 eV band)	20			
	7.7 eV band	80[k]; 55[l]			
benzene	4.7 eV band	60			
	7 eV band	190			

The accuracy of these values is estimated to be within 30%. The reproducibility, however, is often much better (within 10%).

a. This process has been chosen to normalize the cross sections on the measurements of Rapp and Englander-Golden (1965).
b. Maier-Leibnitz (1935).
c. Value for energies lower than 0.5 eV above threshold.
d. Value for energies higher than 0.5 eV above threshold.
e. Rapp and Englander-Golden (1965).
f. Craggs, Thorburn and Tozer (1957).
g. Buchel'nikova (1959).
h. Schulz (1962[b]).
i. Rapp and Briglia (1965).
k. Value for energies lower than 0.5 eV above threshold.
l. Value for energies higher than 0.5 eV above threshold.

SAMENVATTING

De botsing van lage-energie (1 – 30 eV) electronen met moleculen kan aanleiding geven tot verschillende processen, waarvan enkele in dit proefschrift nader zijn bestudeerd. De aandacht was vooral gericht op de aanslag van electronenbeweging en van vibraties, de vorming van positieve ionen en het invangen van electronen door moleculen. Dit laatste proces geeft vaak aanleiding tot dissociatie van het molecuul.

Voor de bestudering van het effect van de wisselwerking van bijna mono-energetische electronen met moleculen is een energiespectrometer gebouwd (hoofdstuk 3). De niet-elastisch verstrooide electronen worden op energie geselecteerd en opgevangen. Het apparaat is speciaal geschikt voor het bestuderen van overgangen waarbij de energie van het opvallende electron juist iets groter is dan de benodigde aanslagenergie.
Hoofdstuk 4 laat een aantal aanslagspectra zien, die met electronenbotsingen bepaald zijn. In deze spectra is het aantal niet-elastisch verstrooide electronen uitgezet als functie van het energieverlies van deze electronen. Dit energieverlies is practisch gelijk aan de energie van de opvallende electronen. Moleculen die bij 150°C een dampdruk hebben die groter is dan 0,01 mm Hg, kunnen gemakkelijk worden gemeten. De spectrometer kan echter tot 350°C verhit worden voor het bestuderen van verbindingen, die bij kamertemperatuur een zeer kleine vluchtigheid bezitten. Speciale aandacht is besteed aan de energie-ijking, daar deze van groot belang is voor een juiste toekenning van de waargenomen overgangen. Een nauwkeurigheid van 0,05 eV kan worden bereikt. De nadelige invloed van ruimtelading op het oplossend vermogen van de spectra is sterk verminderd door het gebruik van zeer kleine electronenstromen (orde van 10^{-9} A). Met een gevoelige detector worden de niet-elastisch verstrooide electronen gemeten (stromen van 10^{-12} – 10^{-16} A).
Het uiterlijk van de aanslagspectra is hetzelfde als dat van ultraviolet absorptiemetingen maar de selectieregels voor de overgangen zijn volledig verschillend. Dit is onder andere een gevolg van het feit dat het opvallende electron kan worden ingevangen in het molecuul, terwijl een electron van dit molecuul wordt verstrooid. Deze uitwisseling kan leiden tot de vorming van een triplet toestand. Zo worden zelfs voor alkanen intensieve singulet-tripletovergangen waargeno-

men. Met andere methoden is het nooit gelukt de ligging van deze tripletniveaus vast te stellen.
Ook is het mogelijk met deze botsingsproeven dissociatie-energieën en electronenaffiniteiten in vacuum te bepalen. De energie-spectrometer werd ingericht voor het bepalen van absolute waarden van de werkzame doorsneden van de aanslag van moleculen. In hoofdstuk 5 worden de resultaten van een aantal absolute metingen getoond. Tot op heden waren geen absolute waarden bekend, hoewel deze van groot belang zijn voor de theoretische interpretatie van drempelprocessen (hoofdstuk 2).

References

Andrick, D. and H. Ehrhardt, Z. Phys., **192** (1966) 99.

Asundi, R.K., Proc. 6th Int. Conf. Ion. Gases, **I** (1963) 29.

Baranger, E. and E. Gerjuoy, Phys. Rev., **106** (1957) 1182.

Barnes, E.E. and W.T. Simpson, J. Chem. Phys., **39** (1963) 670.

Bauer, E. and C.D. Bartky, J. Chem. Phys., **43** (1965) 2466.

Benesch, W., J.T. Vanderslice, S.G. Tilford and P.G. Wilkinson, Astrophys. J., **143** (1966) 236.

Berry, R.S., J. Chem. Phys., **38** (1963) 1934.

Berthod, H., J. Chem. Phys., **45** (1966) 1859.

Boness, M.J.W., J.W. Larkin, J.B. Hasted and L. Moore, Chem. Phys. Lett., **1** (1967) 292.

Bowman, C.R. and W.D. Miller, J. Chem. Phys., **42** (1965) 681.

Brongersma, H.H., J.A. v.d. Hart and L.J. Oosterhoff, Nobel Symposium, **5** (1967^a) 211.

Brongersma, H.H. and L.J. Oosterhoff, Chem. Phys. Lett., **1** (1967^b)169.

Buchel'nikova, I.S., Soviet Phys. JETP, **35** (1959) 783.

Burke, P.G. and K. Smith, Rev. Mod. Phys., **34** (1962) 458.

Chen, J.C.Y., J. Chem. Phys., **40** (1964) 3513.

Christophorou, L.G. and R.N. Compton, Health Phys., **13** (1967) 1277.

Compton, R.N., R.H. Huebner, P.W. Reinhardt and L.G. Christophorou, private communication (1967).

Compton, R.N., G.S. Hurst, L.G. Christophorou and P.W. Reinhardt, Report of the Oak Ridge National Laboratory (1966), ORNL-TM-1409.

Craggs, J.D., R. Thorburn and B.A. Tozer, Proc. Roy. Soc. (London), **A240** (1957) 473.

Craggs, J.D. and B.A. Tozer, Proc. Roy. Soc. (London), **A247** (1958) 337.

Dearden, J.C. and W.F. Forbes, Can. J. Chem., **36** (1958) 1362.

Ditchburn, R.W., Proc. Roy. Soc. (London), **A229** (1955) 44.

Dorrestein, R., Physica, **9** (1942) 447.

Dunn, G.H., Phys. Rev. Lett., **8** (1962) 62.

Ehrhardt, H. and U. Erbse, Z. Phys., **172** (1963) 210.

Ehrhardt, H. and F. Linder, Z. Naturf., **22a** (1967) 11.

Ehrhardt, H., F. Linder and G. Meister, Z. Naturf., **20a** (1965) 989.

Ehrhardt, H. and K. Willmann, Z. Phys., **203** (1967) 1.

Evans, D.F., J. Chem. Soc., (1960) 1735.

Feshbach, H., Ann. Phys. (NY), **5** (1958) 357.

Feshbach, H., Ann. Phys. (NY), **19** (1962) 287.

Feshbach, H., Ann. Phys. (NY), **43** (1967) 410.

Fox, R.E., W.M. Hickam,, D.J. Grove and T. Kjeldaas, Rev. Sci. Instr., **26** (1955) 1101.

Fox, R.E., W.M. Hickam, T. Kjeldaas and D.J. Grove, Phys. Rev., **84** (1951) 859.

Franck, J. and G. Hertz, Verh. Deutsch. Phys. Ges., **16** (1914) 457.

Frost, D.C. and C.A. McDowell, Proc. Roy. Soc. (London), **A241** (1957) 194.

Geiger, J. and K. Wittmaack, Z. Naturf., **20a** (1965) 628.

Gryzinski, M., Phys. Rev., **138** (1965) A336.

Harries, W., Z. Phys., **42** (1927) 26.

Hartwig, D. and K. Ulmer, Z. Phys., **173** (1963) 294.

Heideman, H.G.M., C.E. Kuyatt and G.E. Chamberlain, J. Chem. Phys., **44** (1966) 355.

Henderson, J.R. and M. Muramoto, J. Chem. Phys., **43** (1965) 1215.

Henrich, L.R., Astrophys. J., **99** (1944) 59.

Herzberg, G., Molecular spectra and molecular structure **I**, D. van Nostrand Comp. Inc., Princeton, (1950).

Herzberg, G., Molecular spectra and molecular structure **III**, D. van Nostrand Comp. Inc., Princeton, (1966).

Hodges, S.E., J.R. Henderson and J.B. Coon, J. Mol. Spectr., **2** (1958) 99.

Hoyland, J.R. and L. Goodman, J. Chem. Phys., **36** (1962) 21.

Hush, N.S. and J.A. Pople, Trans. Far. Soc., **51** (1955) 600.

Inokuti, M., Isotopes and Radiation, **1** (1958) 82.

Kieffer, L.J., Bibliography of low-energy electron collision cross section data, National Bureau of Standards Miscellaneous Publication **289**, (1967).

Kraus, K.A., Z. Naturf., **16a** (1961) 1378.

Kuppermann, A. and L.M. Raff, Disc. Far. Soc., **35** (1963[a]) 30.

Kuppermann, A. and L.M. Raff, J. Chem. Phys., **39** 1963[b]) 1607.

Lake, J.S. and A.J. Harrison, J. Chem. Phys., **30** (1959) 361.

Lassettre, E.N. and S.A. Francis, J. Chem. Phys., **40** (1964) 1208.

Lassettre, E.N., F.M. Glaser, V.D. Meyer and A. Skerbele, J. Chem. Phys., **42** (1965[b]) 3429.

Lassettre, E.N., V.D. Meyer and M.S. Longmire, J. Chem. Phys., **42** (1965[a]) 807.

Lassettre, E.N., A. Skerbele and V.D. Meyer, J. Chem. Phys., **45** (1966) 3214.

Lenz, F., Vierter Intern. Kongr. f. Elektronenmikroskopie, Berlin 1958, Bd. I., Springer Berlin-Göttingen-Heidelberg, (1960).

Lichten, W., J. Chem. Phys., **26** (1957) 306.

Lombos, B.A., P. Sauvageau and C. Sandorfy, Chem. Phys. Lett., **1** (1967) 42.

Lutskii, A.E. and V.V. Dorofeev, Zhur. Obschei Khim., **27** (1957) 1303.
Lykos, P.G. and R.G. Parr, J. Chem. Phys., **24** (1956) 1166.
Maier-Leibnitz, H., Z. Phys., **95** (1935) 499.
Maier-Leibnitz, H. and H. Sponer, Z. Phys., **89** (1934) 431.
Marmet, P., Can. J. Phys., **42** (1964) 2102.
Matsuzawa, M., J. Phys. Soc. Japan, **18** (1963) 1473.
Melton, C.E. and W.H. Hamill, J. Chem. Phys., **41** (1964) 546.
Meyer, V.D., A. Skerbele and E.N. Lassettre, J. Chem. Phys., **43** (1965) 805.
Moe, G. and A.B.E. Duncan, J. Am. Chem. Soc., **74** (1952) 3140.
Moskowitz, J.W. and M.C. Harrison, J. Chem. Phys., **42** (1964) 1726.
Mott, N.F. and H.S.W. Massey, The theory of atomic collisions, 3rd ed., Clarendon Press, Oxford (1965).
Muschlitz, E.E. and L. Goodman, J. Chem. Phys., **21** (1953) 2213.
Olmsted III, J., Rad. Res., **31** (1967) 191.
Olmsted III, J., A.S. Newton and K. Street Jr., J. Chem. Phys., **42** (1965) 2321.
Pariser, P. and R.G. Parr, J. Chem. Phys., **21** (1953) 767.
Pearse, R.G.W. and A.G. Gaydon, The identification of molecular spectra, Chapman and Hall Ltd., London, (1965).
Rapp, D. and D.D. Briglia, J. Chem. Phys., **43** (1965) 1480.
Rapp, D. and P. Englander-Golden, J. Chem. Phys., **43** (1965) 1464.
Raymonda, J.W. and W.T. Simpson, J. Chem. Phys., **47** (1967) 430.
Read, F.H. and G.L. Whiterod, Proc. Phys. Soc., **85** (1965) 71.
Robin, M.B., R.R. Hart and N.A. Kuebler, J. Chem. Phys., **44** (1966) 1803.
Ross, K.J. and E.N. Lassettre, J. Chem. Phys., **44** (1966) 4633.
Rudberg, E., Proc. Roy. Soc. (London), **A129** (1930) 629.
Sasaki, V.N. and T. Nakao, Proc. Imp. Acad. Japan, **11** (1935) 138.
Schulz, G.J., Phys. Rev., **112** (1958) 150.
Schulz, G.J., Phys. Rev., **116** (1959) 1141.
Schulz, G.J., Phys. Rev., **125** (1962[a]) 229.
Schulz, G.J., Phys. Rev., **128** (1962[b]) 178.
Schulz, G.J., Phys. Rev., **135** (1964[a]) A988.
Schulz, G.J., Phys. Rev., **136** (1964[b]) A650.
Schulz, G.J. and R.E. Fox, Phys. Rev., **106** (1957) 1179.
Schulz, G.J. and H.C. Koons, J. Chem. Phys., **44** (1966) 1297.
Silverman, S.M. and E.N. Lassettre, J. Chem. Phys., **42** (1965[a]) 3420.
Silverman, S.M. and E.N. Lassettre, J. Chem. Phys., **43** (1965[b]) 194.
Simpson, J.A. and S.R. Mielczarek, J. Chem. Phys., **39** (1963) 1606.
Skerbele, A., V.D. Meyer and E.N. Lassettre, J. Chem. Phys., **44** (1966) 4069.

Skerbele, A., M.A. Dillon and E.N. Lassettre, J. Chem. Phys., **46** (1967[a]) 4161.

Skerbele, A., M.A. Dillon and E.N. Lassettre, J. Chem. Phys., **46** (1967[b]) 4162.

Smit, C., H.G.M. Heideman and J.A. Smit, Physica, **29** (1963) 245.

Smith, P.T., Phys. Rev., **36** (1930) 1293.

Stockburger, M., Z. Phys. Chem., **31** (1962) 350.

Sun, H. and G.L. Weissler, J. Chem. Phys., **23** (1955) 1160.

Takayanagi, K. and T. Takahashi, Report of Ionosphere and Space Research Japan, **20** (1966) 357.

Tanaka, J., S. Nagakura and M. Kobayashi, J. Chem. Phys., **24** (1956) 311.

Tate, J.T. and P.T. Smith, Phys. Rev., **39** (1932) 270.

Tilford, S.G. and J.T. Vanderslice, private communication, (1967).

U.V. Atlas of Organic Compounds **1**, Butterworth Chemie Verlag, London, (1966).

Watanable, K., J. Chem. Phys., **26** (1957) 542.

Winters, H.F., J. Chem. Phys., **43** (1965) 926.

Woudenberg, J.P.M. and J.M.W. Milatz, Physica, **8** (1941) 871.

Zelikoff, M. and K. Watanable, J. Opt. Soc. Am. **43** (1953) 756.

Teneinde te voldoen aan de wens van de faculteit der Wiskunde en Natuurwetenschappen volgt hier een kort overzicht van mijn academische studie.

Na het behalen van het einddiploma HBS B aan het Rembrandt Lyceum te Leiden begon ik in september 1958 mijn studie aan de Rijksuniversiteit te Leiden. Het candidaatsexamen in de natuur- en scheikunde met bijvak wiskunde (letter E) legde ik in juni 1962 af. Mijn studie werd voortgezet op de afdeling voor theoretische organische scheikunde van Prof. Dr. L.J. Oosterhoff. Hier werkte ik onder leiding van Dr. H.M. Buck mee aan het onderzoek op het gebied van de fotochemie en van de reacties in sterk zure media. In oktober 1965 legde ik cum laude het doctoraal-examen af in de theoretische organische scheikunde met de bijvakken theoretische natuurkunde en wiskunde.

In juni 1966 begon ik in het F.O.M. Instituut voor Atoom- en Molekuulfysica te Amsterdam met de opbouw van de apparatuur voor het bestuderen van de verstooiing van laag-energetische electronen aan moleculen. Alle experimenten, die in dit proefschrift worden besproken zijn in dit instituut uitgevoerd.
Gedurende de periode juli 1963 - november 1965 was ik als candidaats-assistent in dienst van de Rijksuniversiteit te Leiden. Hierna was ik als doctoraal-assistent in dienst van Z.W.O. (S.O.N.). Sedert oktober 1967 ben ik verbonden aan het Natuurkundig Laboratorium van N.V. Philips Gloeilampenfabrieken te Eindhoven.

De gastvrijheid, die ik in de laatste twee jaren genoten heb in het F.O.M. Instituut voor Atoom- en Molekuulfysica, is van groot belang geweest voor het werk dat in dit proefschrift is beschreven. De directeur van dit instituut Prof. Dr. J. Kistemaker ben ik hiervoor zeer erkentelijk. De stimulerende omgang met het wetenschappelijk en technisch personeel en de hulp die ik van hen ontving heb ik zeer gewaardeerd.

Van de wetenschappelijke medewerkers dank ik in het bizonder de leider van de afdeling voor Massaspectrometrie Dr. Ir. A.J.H. Boerboom. Bij de voorbereiding en de uitvoering van de metingen heeft de samenwerking met de heren W. Kleine, Tj. van der Hauw en H.G. den Harinck veel bijgedragen tot het slagen ervan.
Speciaal vermeld ik de onmisbare steun die bij de constructie van de meetapparatuur geboden werd door de electronische afdeling (onder leiding van de heer P.J. van Deenen) en de instrumentmakerij (onder leiding van de heer A.F. Neuteboom).
De tekeningen werden verzorgd door mej. Benavente, terwijl de heer H.G. den Harinck hier ook een belangrijk aandeel in heeft gehad. Verder bedank ik de heren F. Monterie en Th. van Dijk voor het vele fotografische werk.

De prettige samenwerking met de leden van de theoretische afdeling in Leiden is door mij bizonder op prijs gesteld. Vooral de stimulerende discussies met mevr. Drs. J. van der Hart-van der Hoek heb ik zeer gewaardeerd.
Ik heb het zeer op prijs gesteld, dat ik door een subsidie van ZWO als SON medewerker in staat ben gesteld mij volledig aan dit onderzoek te wijden.

De Directie van het Koninklijke Shell laboratorium te Amsterdam dank ik voor de vele verbindingen van grote zuiverheid die zij voor dit onderzoek hebben willen afstaan.

De Directie van de N.V. Philips Gloeilampenfabrieken ben ik erkentelijk voor hun medewerking bij het voltooien van het proefschrift.

STELLINGEN

1. De bewering van Hudson, dat fosfinen zoals trifenylfosfoniumdifenylmethylide zeer weinig reactief zijn, is onjuist.

   Horner, L. en E. Lingnau, Ann. Chem., **591** (1955) 135.
   Hudson, R.F., Structure and Mechanism in Organo-Phosphorus Chemistry, Academic Press, London, (1965) 85 en 221.

2. De wijze, waarop Tai en Allinger rotatiesterkten van ketonen berekenen, is aan bedenkingen onderhevig.

   Tai, J.C. en N.L. Allinger, J. Am. Chem. Soc., **88** (1966) 2179.

3. Het is moeilijk om met een energiespectrometer, zoals beschreven in dit proefschrift, aanslagspectra te verkrijgen van moleculen die een groot dipoolmoment hebben in de eerste aangeslagen toestand(en). Om aan deze beperking van de apparatuur tegemoet te komen verdient het aanbeveling een energieselector te construeren, waarmee niet-elastisch verstrooide electronen met een energie van enkele electronvolts geselecteerd kunnen worden.

   Crawford, O. en A. Dalgarno, Chem. Phys. Lett., **1** (1967) 23.
   Dit proefschrift, hoofdstuk 3.

4. Het door Verspyck Mijnssen uit de tulpenbol geisoleerde allergeen vertoont meer gelijkenis met het inactieve dan met het actieve tuliposide A van Tschesche et al. .

   Brongersma–Oosterhoff, U.W., Rec. Trav. Chim., **86** (1967) 705.
   Tschesche, R., F.J. Kammerer, G. Wulff en F. Schönbeck, Tetrahedron Lett., **6** (1968) 701.
   Verspyck Mijnssen, G.A.W., Dermatologica, **134** (1967) 379.

5. De formule voor de eerste orde exchange benadering, die Bell, Eissa en Moiseiwitsch afleiden voor de tripletaanslag van helium door electronen, is in feite een bizonder geval van de Born-benadering van het optisch potentiaalmodel voorgesteld door Mittleman.

   Bell, K.L., H. Eissa en B.L. Moiseiwitsch, Proc. Phys. Soc., **88** (1966) 57.
   Joachain, C.J. en M.H. Mittleman, Phys. Rev., **140** (1965) A432.
   Mittleman, M.H., Phys. Rev., **122** (1961) 1930.

6. Het opnemen van een ^{17}O kernspinresonantie spectrum van sulfeenzuren zal mogelijk uitsluitsel kunnen geven over de positie van het waterstofatoom.

Fluck, E., Die kernmagnetische Resonanz und ihre Anwendung in der anorganischen Chemie, Springer-Verlag, Berlin-Göttingen-Heidelberg, (1963) 195.
Shelton, J.R. en K.E. Davis, J. Am. Chem. Soc., **89** (1967) 718.

7. De conclusie van Beyer en Welger, dat de moleculaire fluorescentie van H_2 in het gebied van de Lyman-α overgang te verwaarlozen is ten opzichte van atomaire fluorescentie, is onjuist.

Beyer, K.D. en K.H. Welger, Z. Naturf., **19a** (1967) 1161.
Geiger, J., Z. Phys., **181** (1964) 413.
Reich, H.J. en H. Schmoranzer, Phys. Lett., **9** (1964) 127.

8. Voor het volgen van reacties, waarbij gassen en (of) gemakkelijk te verdampen verbindingen worden gevormd of verdwijnen, kan het aanbeveling verdienen een energiespectrometer zoals beschreven in dit proefschrift (hoofdstuk 3) bij de analyse in te schakelen.

9. De beschieting van een mengsel van azuleen en deuterium met langzame electronen zou gebruikt kunnen worden voor het bereiden van bepaalde deutero-azulenen. Met behulp van deze deuteroazulenen zou men vervolgens een aanslagspectrum van azuleen kunnen verkrijgen.

Dit proefschrift, hoofdstuk 4.

10. Het verdient aanbeveling meer gebruik te maken van fysische hulpmiddelen bij het opleiden en selecteren van wedstrijdroeiers. Dit geldt in het bizonder voor roeiverenigingen die niet over ervaren coaches beschikken.

H.H. Brongersma

Leiden, 13 mei 1968